

Global Analysis of Piecewise Linear Systems Using Impact Maps and Quadratic Surface Lyapunov Functions

Jorge M. Gonçalves^{*†‡}, Alexandre Megretski[†], Munther A. Dahleh[‡]
Department of EECS, Room 35-401
MIT, Cambridge, MA, USA
jmg@mit.edu, ameg@mit.edu, dahleh@mit.edu

January 29, 2004

Abstract

In this paper we develop an entirely new constructive global analysis methodology for a class of hybrid systems known as *Piecewise Linear Systems* (PLS). This methodology consists of inferring global properties of PLS solely by studying their behavior at switching surfaces associated with PLS. The main idea is to analyze *impact maps*, i.e., maps from one switching surface to the next switching surface. These maps are proven globally stable by constructing quadratic Lyapunov functions on switching surfaces. Impact maps are known to be “unfriendly” maps in the sense that they are highly nonlinear, multivalued, and not continuous. We found, however, that an impact map induced by an LTI flow between two switching surfaces can be represented as a linear transformation analytically parametrized by a scalar function of the state. Moreover, level sets of this function are convex subsets of linear manifolds. This representation of impact maps allows the search for *quadratic surface Lyapunov functions* (SuLF) to be done by simply solving a set of LMIs. Global asymptotic stability, robustness, and performance of limit cycles and equilibrium points of PLS can this way be efficiently checked. These new results were successfully applied to certain classes of PLS: relay feedback, on/off and saturation systems. Although this analysis methodology yields only sufficient criteria of stability, it has shown to be very successful in globally analyzing a large number of examples with a locally stable limit cycle or equilibrium point. In fact, it is still an open problem whether there exists an example with a globally stable limit cycle or equilibrium point that cannot be successfully analyzed with this new methodology. Examples analyzed include systems of relative degree larger than one and of high dimension, for which no other analysis methodology could be applied. This success in globally analyzing certain classes of PLS has shown the power of this new methodology, and suggests its potential toward the analysis of larger and more complex PLS.

^{*}Research supported in part by the Portuguese Science and Technology Foundation under the program “PRAXIS XXI”.

[†]Research supported in part by the NSF under grants ECS-9410531, ECS-9796099, and ECS-9796033, and by the AFOSR under grants F49620-96-1-0123 and F49620-00-1-0096

[‡]Research supported in part by the NSF under grant ECS-9612558 and by the AFOSR under grant AFOSR F49620-95-0219 and F49620-99-1-0320.

1 Introduction

It is often possible to linearize a system, i.e., to obtain a linear representation of its behavior. That representation approximates the true dynamics well in a small region. For example, the true equations of the pendulum are never linear but, for very small deviations (a few degrees) they may be satisfactorily replaced by linear equations. In other words, for small deviations, the pendulum may be replaced by a harmonic oscillator. This ceases to hold, however, for large deviations and, in dealing with these, one must consider the nonlinear equation itself and not merely a linear substitute. In this work, we are interested in a class of nonlinear systems known as *piecewise linear systems* (PLS). PLS are characterized by a finite number of linear dynamical models together with a set of rules for switching among these models. Therefore, this model description causes a partitioning of the state space into cells. These cells have distinctive properties in that the dynamics within each cell are described by linear dynamic equations. The boundaries of each cell are in effect switches between different linear systems. Those switches arise from the breakpoints in the piecewise linear functions of the model.

The reason why we are interested in studying this class of systems is to capture discontinuity actions in the dynamics from either the controller or system nonlinearities. On one hand, a wide variety of physical systems are naturally modeled this way due to real-time changes in the plant dynamics like collisions, friction, saturation, walking robots, etc. On the other hand, an engineer can introduce intentional nonlinearities to improve system performance, to effect economy in component selection, or to simplify the dynamic equations of the system by working with sets of simpler equations (e.g., linear) and switch among these simpler models (in order to avoid dealing directly with a set of nonlinear equations).

Although widely used, just a few years ago there were very few results available to analyze PLS. The research in [9] took the first step in changing this. There, piecewise quadratic Lyapunov functions are constructed by solving a set of linear matrix inequalities (LMIs). There are, however, several problems with this approach, discussed in detail in section 2, that motivate the development of new tools.

In [6], we introduced an entirely new methodology to globally analyze symmetric unimodal limit cycles¹ of relay feedback systems. The idea consisted in finding a quadratic Lyapunov function on a switching surface that can be used to prove that the associated Poincaré map is contracting in some sense.

This paper generalizes the ideas from [6] to globally analyze PLS. In a similar way, the main idea consists of finding quadratic Lyapunov functions on associated switching surfaces that can be used to prove that *impact maps*, i.e., maps from one switching surface to the next switching surface, are contracting in some sense. The notion of an impact map can be thought as a generalization of a Poincaré map. The novelty of this work comes from expressing impact maps induced by an LTI flow between two hyperplanes as linear transformations analytically parametrized by a scalar function of the state. Furthermore, level sets of this function are convex subsets of linear manifolds with dimension lower than that of the switching surfaces. This allows us to search for *quadratic surface Lyapunov functions* (SuLF) by solving sets of LMIs using efficient computational algorithms. Contractions of certain impact maps of the system can then be used to conclude about global stability, robustness, and performance of PLS.

We will show that this new methodology can be used to not only globally analyze limit

¹A limit cycle is *unimodal* if it only switches twice per cycle.

cycles but also equilibrium points of PLS. For that, we analyze on/off and saturation systems (sections 6 and 7, respectively), including those with unstable nonlinearity sectors for which classical methods like Popov criterion, Zames–Falb criterion [20], IQCs [3, 10, 12, 13], fail to analyze. In addition, the results in [5] and [4, chapter 8] show that this methodology can also be efficiently used to analyze robustness and performance of PLS. Thus, the success in globally analyzing stability, robustness, and performance of certain classes of PLS has shown the power of this new methodology, and suggests its potential toward the analysis of larger and more complex PLS.

This paper is organized as follows. In the next section, we motivate the need for new analysis tools for PLS by explaining how available methods can be inefficient or even unable to analyze many PLS. In section 3, we introduce the notion of impact maps, which are simply maps between two switching surfaces. We show that impact maps induced by an LTI flow can be represented as linear transformations analytically parametrized by a scalar function of the state. This, in turn, allows us to relax the problem of checking quadratic stability of impact maps to solving a set of LMIs, as explained in section 4. The results developed in sections 3 and 4 are applied to globally analyze asymptotic stability of on/off and saturation systems. These can be found in sections 6 and 7, respectively. Section 8 shows how less conservative global stability conditions can be obtained. Conclusions and future work are discussed in section 9 and, finally, technical details are considered in appendix.

2 Motivation

As discussed in introduction, there exist several tools to analyze PLS. One of the most important consists of constructing piecewise quadratic Lyapunov functions in the state space [8, 9, 15]. This method relaxes the problem to a solution of a finite dimensional set of LMIs. There are, however, several drawbacks with this approach that motivates the need for alternative methods to analyze PLS. These drawbacks are:

- Piecewise quadratic Lyapunov functions in the state space cannot be constructed to analyze limit cycles.
- For most PLS, it is not possible to construct piecewise quadratic Lyapunov functions with just the given natural partition of the system. In order to improve flexibility of the method proposed in [9], a subdivision of partitions is typically necessary. The analysis method, however, is efficient only when the number of partitions required to prove stability is small. Example 2.1 shows that even for second order systems, the construction of piecewise quadratic Lyapunov functions can be computationally intractable due to the large number of partitions in the state space required for the analysis.
- In general, for systems of order higher than 3, it is extremely hard to obtain a refinement of partitions in the state-space to efficiently analyze PLS using piecewise quadratic Lyapunov functions. In other words, the method does not scale well with the dimension of the system. In fact, only a few and specific examples of PLS of order higher than 3 analyzed with this method have been reported.
- Existence of piecewise quadratic Lyapunov functions implies exponential stability of the system. Thus, the approach proposed in [9] cannot prove asymptotic stability of PLS when these are not exponentially stable.

Example 2.1 Consider the PLS in figure 1 composed of two linear subsystems. On the left side of the vertical axis— x_2 axes—we have an unstable linear system and on the right side we have a stable linear system parametrized by $\epsilon > 0$. In this simple second order PLS, we are interested in showing that the origin is globally asymptotically stable.

$$\dot{x} = \begin{bmatrix} 1 & 1 \\ -1 & 1 \end{bmatrix} x \quad \begin{array}{c} \uparrow x_2 \\ \bullet \\ \downarrow \\ 0 \\ \rightarrow x_1 \end{array} \quad \dot{x} = \begin{bmatrix} -1-\epsilon & 1 \\ -1 & -1-\epsilon \end{bmatrix} x \quad \epsilon > 0$$

Figure 1: PLS composed of an unstable and a stable linear systems

For this system, there is no global quadratic Lyapunov function. We then turn to find piecewise quadratic Lyapunov functions. As seen in the figure, the PLS divides the state space in two equal partitions. However, as we will see, in order to construct piecewise quadratic Lyapunov functions, a much larger number of partitions is required to prove stability of the origin.

We start with just the natural partition of the system. Using the software developed by [9], no piecewise quadratic Lyapunov functions can be found this way. This was expected from the same reason there is no global quadratic Lyapunov function. A more refined partition of the state space is then required. This refinement must be supplied to the software. We decided to partition the state space with lines through the origin, including the x_2 axes, and with each separated by an angle of $2\pi/k$ radius, where k is a positive integer. This resulted in k equally sized partitions (see the left of figure 2 for $k = 16$). For a given $\epsilon > 0$, we tried successively $k = 2, 4, 8, 16, 32, \dots$ until we could successfully analyze the system. The table in the center of figure 2 shows the smallest k required to analyze the system as a function of ϵ .

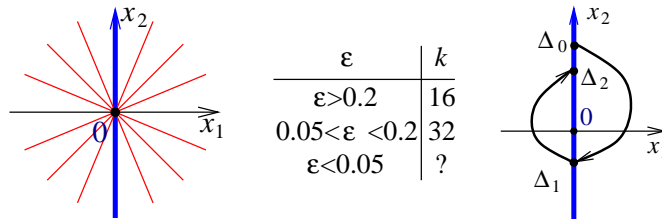


Figure 2: State space partitioned in 16 equal cells (left); Maps from one switch to the next switch (right)

This table clearly shows that as ϵ decreases, the required number of partitions for the analysis of the PLS increases. For $\epsilon < 0.05$, the number of required partitions is very high and it becomes computationally intractable to prove stability of the origin using this method. Note that even for large values of ϵ , the number of required partitions is 16, although the original system is only divided in 2 partitions.

Note that this system is easily analyzed using SuLF without requiring extra switching surfaces. In fact, it is easy to show that the maps from one switch to the next are quadratically stable for any $\epsilon > 0$ (see the right side of figure 2).

Let A_1 be the linear matrix for the stable system and A_2 for the unstable one. For a given $\epsilon > 0$, both maps around the origin can be expressed as $\Delta_1 = H_1(t_1)\Delta_0$ and $\Delta_2 = H_2(t_2)\Delta_1$, where $H_i(t_i) = e^{A_i t_i}$, for $i = 1, 2$. Since Δ_i belong to the x_2 axis, these

can be parametrized by $\Delta_i = \Pi\delta_i$, where $\Pi' = \begin{pmatrix} 0 & 1 \end{pmatrix}$ and $\delta_i \in \mathbb{R}$. Let $F_i(t_i) = \Pi'H_i(t_i)\Pi$. Global asymptotic stability of the origin follows if both maps are quadratically stable. Thus, we need to find $p_0 > 0$ and $p_1 > 0$ such that

$$\begin{aligned} F_1'(t_1)p_1F_1(t_1) &< p_0 && \text{for all switching times } t_1 \\ F_2'(t_2)p_0F_2(t_2) &< p_1 && \text{for all switching times } t_2 \end{aligned}$$

Let $q = p_1/p_0 > 0$. Since the switching times are always $t_i = \pi$ for any initial condition on the switching surface, stability follows if there exists a $q > 0$ such that $[F_1(\pi)]^2 q < 1$ and $[F_2(\pi)]^2 < q$, or

$$[F_2(\pi)]^2 < q < \frac{1}{[F_1(\pi)]^2}$$

Since, for any $\epsilon > 0$, $[F_2(\pi)F_1(\pi)]^2 = e^{-2\pi\epsilon} < 1$, the following q

$$q = \frac{[F_2(\pi)F_1(\pi)]^2 + 1}{2[F_1(\pi)]^2} = \frac{e^{-2\pi\epsilon} + 1}{2e^{2\pi}}$$

satisfies the stability conditions. Therefore, the origin is globally asymptotically stable for all $\epsilon > 0$. ■

The construction of piecewise quadratic Lyapunov functions for PLS proposed in [9] imposes continuity of the the Lyapunov functions along switching surfaces. This means that the intersection of two Lyapunov functions with a switching surface—one from each side—defines a unique quadratic Lyapunov function on the switching surface. Hence, existence of piecewise quadratic Lyapunov functions guarantee the existence of SuLF. The converse, however, is not true. For instance, SuLF exist to analyze limit cycles [6], but no piecewise quadratic Lyapunov functions exist in the state space.

Analysis of PLS at switching surfaces requires the understanding of system trajectories. When a trajectory leaves a switching surface it will either not switch again or switch in finite time (see figure 3). If the trajectory *does not* switch again then its behavior from thereon is simply governed by a linear system. Thus, linear analysis tools can be applied to this trajectory to check whether or not this will converge to an equilibrium point.

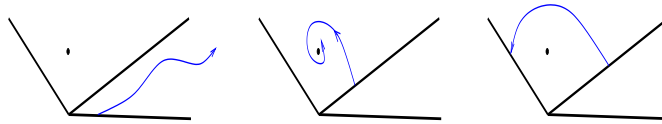


Figure 3: Possible scenarios for a trajectory entering a cell: not convergent or unstable, stable, and switching trajectory

Things become more interesting if a trajectory leaving a switching surface *does* switch in finite time. The immediate question is: what happens to the trajectory after it switches? Will it switch again? Will it converge to some equilibrium point or limit cycle? These are the type of questions we address in this paper. Thus, the first step will be to fully understand a single map from one switching surface to the next switching surface (sections 3 and 4). Then, PLS can be analyzed by combining the analysis of all switching maps associated with the system (section 5).

Analysis of nonlinear systems at manifolds has been used by many researchers. The so-called *Poincaré map* was introduced in order to reduce the study of an n -dimensional

system to a discrete $n - 1$ -dimensional system in a manifold (see, for example, [11] for an introduction to Poincaré maps). The problem with Poincaré maps is that they are typically nonlinear, not continuous, and multivalued. Thus, global analysis of PLS is rarely done using these maps. This paper explains how these difficulties inherent to Poincaré maps can be overcome to allow such maps to globally analyze PLS.

Note that all the drawbacks discussed above associated with the method proposed by [9], based on piecewise quadratic Lyapunov functions, are not an issue for the classes of PLS analyzed so far using SuLF. First, SuLF can analyze both limit cycles [6] and equilibrium points (sections 6 and 7). Second, it is sufficient to consider only the natural partition of the system, with no extra complexity added. Third, our new method scales with the dimension of the system, and, finally, SuLF can be used to prove global asymptotic stability of PLS that are not exponentially stable (see example 7.3).

3 Impact maps

In order to analyze PLS using SuLF, we first need to understand the behavior of the system as this flows from one switching surface to the next switching surface. A useful notion that we will use throughout this paper is that of *impact map*. An impact map is simply a map from one switching surface to the next switching surface. Only after we understand the nature of a single impact map can we look at a PLS as a whole, by combining all impact maps associated with the PLS, to conclude about stability, robustness, and performance properties of the system.

Consider the following affine linear time-invariant system

$$\dot{x} = Ax + B \tag{1}$$

where $x \in \mathbb{R}^n$, $A \in \mathbb{R}^{n \times n}$, and $B \in \mathbb{R}^n$. Note that we are not imposing any kind of restrictions on A . The matrix A is allowed to have stable, unstable, and pure imaginary eigenvalues. Assume (1) is part of some PLS, and that (1) is defined on some open polytopical set $X \subset \mathbb{R}^n$. Assume also a trajectory just arrived in a subset of the boundary² of X belonging to

$$S_0 = \{x \in \mathbb{R}^n : C_0x = d_0\}$$

and the system switches to (1). In this paper, we are interested in studying the impact map from some subset of S_0 to some subset of

$$S_1 = \{x \in \mathbb{R}^n : C_1x = d_1\}$$

also in the boundary of X . In this scenario, some subsets of S_0 and S_1 are switching surfaces of the PLS.

By a solution of (1) we mean a function x defined on $[0, t]$, with $x(0) \in S_0$, $x(t) \in S_1$, $x(\tau) \in \bar{X}$ on $[0, t]$ ³, and satisfying (1). In this case, t is a *switching time* of the solution x of (1) and we say a *switch* occurs at $x(t)$.

Let S_0^d be some polytopical subset of S_0 where any trajectory starting at S_0^d satisfies $x(t) \in S_1$, for some finite $t \geq 0$, and $x(\tau) \in \bar{X}$ on $[0, t]$. Let also $S_1^a \subset S_1$ be the set of those points $x_1 = x(t)$. The set S_1^a can be seen as the image set of S_0^d . We call S_0^d the *departure set* in S_0 and S_1^a the *arrival set* in S_1 (see figure 4).

²The *boundary* of X is the set of all limit points p of X such that $p \notin X$.

³ \bar{X} denotes the *closure* of X , i.e, the set $\bar{X} = X \cup \{p \mid p \text{ is a limit point of } X\}$.

We are interested in studying the impact map, induced by (1), from $x_0 \in S_0^d$ to $x_1 \in S_1^a$. Since both x_0 and x_1 belong to switching surfaces, they can be parametrized in their respective hyperplanes. For that, let $x_0 = x_0^* + \Delta_0$ and $x_1 = x_1^* + \Delta_1$, where $x_0^* \in S_0$, $x_1^* \in S_1$, and Δ_0, Δ_1 are any vectors such that $\Delta_0 \in S_0^d - x_0^*$ and $\Delta_1 \in S_1^a - x_1^*$. In this case, $C_0\Delta_0 = C_1\Delta_1 = 0$. Note that x_0^* and x_1^* do not need to belong to S_0^d and S_1^a , respectively. In fact, as we will see later, in many cases it will be convenient to choose $x_0^* \in S_0$ so that $x_0^* \notin S_0^d$. Define also $x_0^*(t)$ as the trajectory of (1), starting at x_0^* , for all $t \geq 0$. The impact map of interest reduces to the map from Δ_0 to Δ_1 (see figure 4).

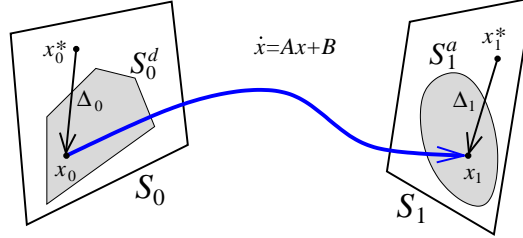


Figure 4: Impact map from $\Delta_0 \in S_0^d - x_0^*$ to $\Delta_1 \in S_1^a - x_1^*$

Note that, in general, the impact map from $\Delta_0 \in S_0^d - x_0^*$ to $\Delta_1 \in S_1^a - x_1^*$ defined above is multivalued and not continuous. This is illustrated in the following example.

Example 3.1 Consider a 3rd-order system given by

$$\dot{x} = \begin{pmatrix} -1 & 0 & 0 \\ 0 & -2 & 0 \\ 0 & 0 & -3 \end{pmatrix} x + \begin{pmatrix} 1 \\ 1 \\ 1 \end{pmatrix}$$

with the switching surfaces defined above given by $C_0 = C_1 = [-2 \ 2 \ 1]$, and $d_0 = 0.5$, $d_1 = -0.5$. Let $X = \{x \mid d_1 < C_1x(t) < d_0\}$. In the state space, the switching surfaces are parallel to each other. Let $x(0) = [-0.7 \ -4.35 \ 7.8]'$ $\in S_0$. The resulting $C_1x(t)$ can be seen on the left of figure 5.

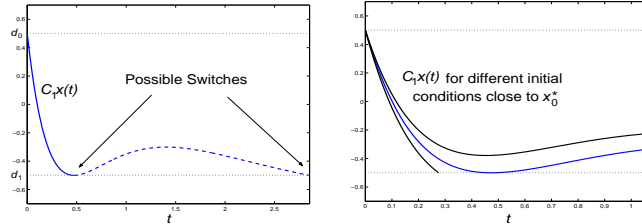


Figure 5: Existence of multiple solutions (left); Map from Δ_0 to Δ_1 is not continuous (right)

When $t \approx 0.47$, $C_1x(t) = d_1$ and $C_1\dot{x}(t-0) = 0$. At this point, the trajectory can return to X (dashed trajectory), or it can switch. This means that a switch can occur at either $t = 0.47$ or $t = 2.85$, showing that the impact map is multivalued.

Now, let $x_0^* = x(0)$ and $x_1^* = x(0.47)$. The impact map from Δ_0 to Δ_1 , as defined above, is also not continuous since in a small enough neighborhood $\mathcal{W} \subset S_1$ of x_1^* , there is no neighborhood $\mathcal{W}_0 \subset S_0$ of x_0^* such that every point in \mathcal{W}_0 is mapped in \mathcal{W} (see the right of figure 5). In this figure, we have two initial conditions in a small neighborhood of x_0^* . One of these (in the figure, the one on the left) switches “close” to x_1^* while the other (the one of the right) switches “far” from x_1^* . ■

Definition 3.1 Let $x(0) = x_0^* + \Delta_0$. Define t_{Δ_0} as the set of all times $t_i \geq 0$ such that the trajectory $x(t)$ with initial condition $x(0)$ satisfies $C_1x(t_i) = d_1$ and $x(t) \in \bar{X}$ on $[0, t_i]$. Define also the set of *expected switching times* of the impact map from $\Delta_0 \in S_0^d - x_0^*$ to $\Delta_1 \in S_1^a - x_1^*$ as

$$\mathcal{T} = \left\{ t \mid t \in t_{\Delta_0}, \Delta_0 \in S_0^d - x_0^* \right\}$$

For instance, in example 3.1, $t_{\Delta_0} = \{0.47, 2.85\}$ for the initial condition $x(0)$.

For an impact map, once an initial condition $\Delta_0 \in S_0^d - x_0^*$ is given, in order to find an image $\Delta_1 \in S_1^a - x_1^*$, we must first find an associated switching time t . Solving for t , however, involves solving a transcendental equation. Solution to such equations cannot, in general, be written in closed form, and numerical procedures are typically the only way to solve for t . Once a switching time is found, we can finally find the corresponding Δ_1 .

Thus, in general, impact maps are highly nonlinear, multivalued, and not continuous. This “non-friendly” nature of impact maps is the main reason why global analysis of PLS has not been done before using SuLF. The following result, however, shows that this map is not as “bad” as it looks, and opens the door to analysis of PLS at switching surfaces.

Theorem 3.1 *Assume $C_1x_0^*(t) \neq d_1$ for all $t \in \mathcal{T}$. Define*

$$w(t) = \frac{C_1e^{At}}{d_1 - C_1x_0^*(t)}$$

and let

$$H(t) = e^{At} + (x_0^*(t) - x_1^*)w(t)$$

Then, for any $\Delta_0 \in S_0^d - x_0^*$ there exists a $t \in \mathcal{T}$ such that the impact map is given by

$$\Delta_1 = H(t)\Delta_0 \tag{2}$$

Such $t \in t_{\Delta_0}$ is the switching time associated with Δ_1 .

This theorem says that maps between switching surfaces, induced by an LTI flow, can be represented as linear transformations analytically parametrized by a scalar function of the state. At first, equation (2) may not seem of great help in analyzing the impact map. Δ_1 is a linear function of Δ_0 and a nonlinear function of the switching time t . The switching time, however, is a nonlinear function of Δ_0 and a transcendental equation still needs to be solved in order to find t . Thus, by this reasoning, it seems (2) is saying that Δ_1 is a nonlinear function of Δ_0 . But, that we already knew.

This is, however, just one way of thinking about (2). Fortunately, there is another way to approach equation (2). Assume, for now, the switching time t is fixed. The result: the impact map (2) would be linear! So, the question is: what does it mean to have the switching time t fixed? In other words, what are the set of points $x_0^* + \Delta_0$ in the switching surface S_0 such that every point in that set has a switching time of t ? In that set, the impact map (2) is linear.

It turns out that the set of points in S_0^d that have a switching time of t is a convex subset of a linear manifold of dimension $n - 2$ (see figure 6). Let S_t be that set, that is, the set of points $x_0^* + \Delta_0 \in S_0^d$ such that $t \in t_{\Delta_0}$. In other words, a trajectory starting at $x_0 \in S_t$ satisfies both $x(\tau) \in \bar{X}$ on $[0, t]$, and $C_1x(t) = d_1$. Note that since the impact map is multivalued, a point in S_0^d may belong to more than one set S_t . In fact, in example 3.1, there existed a point in S_0^d that belonged to both $S_{0.47}$ and $S_{2.85}$.

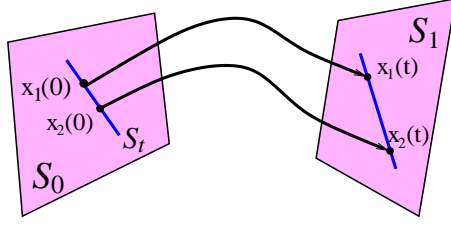


Figure 6: Every point in S_t has a switching time of t

Note also that, as $t \in \mathcal{T}$ changes, S_t covers every single point of S_0^d , i.e., $S_0^d = \{x \mid x \in S_t, t \in \mathcal{T}\}$. This follows since every point $\Delta_0 \in S_0^d - x_0^*$ can switch for the first time at S_1^a , and therefore t_{Δ_0} is always a nonempty set. These results can all be summarized in the following corollary.

Corollary 3.1 *Under the assumptions of theorem 3.1, for a given $t \in \mathcal{T}$, the impact map from $\Delta_0 \in S_t - x_0^*$ to $\Delta_1 \in S_1 - x_1^*$, given by $\Delta_1 = H(t)\Delta_0$, is a linear map. Moreover, S_t is a subset of a linear manifold of dimension $n - 2$, and $S_0^d = \{x \mid x \in S_t, t \in \mathcal{T}\}$.*

As we will see in section 4, this result is fundamental in the analysis of PLS using SuLF. It allows us to find conditions in the form of LMIs that, when satisfied, guarantee stability, robustness, and performance of PLS.

Before moving into the proofs, it is important to understand the meaning of the assumption in theorem 3.1. This says the trajectory $x_0^*(t)$ cannot intersect the switching surface S_1 for all $t \in \mathcal{T}$. Note that we have not made any assumptions on x_0^* (the initial condition of $x_0^*(t)$), except for the fact that $x_0^* \in S_0$. Thus, a careful choice of $x_0^* \in S_0$ may be enough to have the assumption satisfied (see sections 6 and 7).

There are, however, cases where either x_0^* cannot be freely chosen (like in [6]) or there is simply no choice of $x_0^* \in S_0$ that satisfies the assumption. This means there exist at least one $t_s \in \mathcal{T}$ such that $C_1 x_0^*(t_s) = d_1$. In such cases, the results in this paper still hold but with a slightly more complicated proof. For some PLS like RFS [6], $w(t)$ at $t = t_s$ is defined as the limit when $t \rightarrow t_s$ (see [6] for details). If this is not the case, at $t = t_s$ the impact map can still be written as a linear transformation but parametrized by an extra variable, i.e., $\Delta_1 = H_s(t_s, \delta)\Delta_0$, with $\Delta_0 \in S_{t_s}$.

Proof of theorem 3.1: We start by expressing Δ_1 as function of Δ_0 and t , the switching time associated with Δ_1 . Let $x(0) = x_0 \in S_0^d$. Integrating the differential equation (1) gives

$$x_1 = e^{At}x_0 + \int_0^t e^{A(t-\tau)}Bd\tau$$

Since $x_i = x_i^* + \Delta_i$, $i = 0, 1$,

$$\begin{aligned} \Delta_1 &= e^{At}\Delta_0 + e^{At}x_0^* + \int_0^t e^{A(t-\tau)}Bd\tau - x_1^* \\ &= e^{At}\Delta_0 + x_0^*(t) - x_1^* \end{aligned}$$

From the fact $C_1\Delta_1 = 0$ and $C_1x_1^* = d_1$ we get

$$C_1e^{At}\Delta_0 = d_1 - C_1x_0^*(t) \tag{3}$$

Since, by assumption, $C_1 x_0^*(t) \neq d_1$ for all $t \in \mathcal{T}$, the last expression can be written as

$$w(t)\Delta_0 = 1 \quad (4)$$

which means Δ_1 reduces to

$$\Delta_1 = e^{At}\Delta_0 + (x_0^*(t) - x_1^*)w(t)\Delta_0$$

which proves the desired result. \blacksquare

Note that if A is invertible, $x_0^*(t)$ can be written as $x_0^*(t) = e^{At}(x_0^* + A^{-1}B) - A^{-1}B$.

Proof of corollary 3.1: The only thing left to prove is that S_t is a subset of a linear manifold of dimension $n - 2$. Let $x_0 = x_0^* + \Delta_0 \in S_t$. Since $C_1 x(t) = d_1$, Δ_0 must satisfy equation (3). Also, $C_0 \Delta_0 = 0$ since $\Delta_0 \in S_0 - x_0^*$. Therefore, since both equalities are linear on Δ_0 , $S_t - x_0^*$ has at most dimension $n - 2$ and is a subset of a linear manifold. \blacksquare

4 Quadratic surface Lyapunov functions

As explained before, there has been some results in constructing piecewise quadratic Lyapunov functions for PLS. Although these results are able to analyze equilibrium points of certain classes of PLS, many important PLS cannot be analyzed this way because they either have limit cycles or the method is computationally too expensive.

An alternative to construct Lyapunov functions in the state space is to construct Lyapunov functions on switching surfaces (SuLF). Define then two quadratic Lyapunov functions on the switching surfaces S_0^d and S_1^a . Respectively, let V_0 and V_1 be given by

$$V_i(x) = x'P_i x - 2x'g_i + \alpha_i \quad (5)$$

where $P_i > 0$, for $i = 0, 1$. These are Lyapunov candidates defined on the switching surfaces with parameters $P_i > 0$, g_i , and α_i , to be found.

Next, we want to show an impact map from $S_0^d \subset S_0$ to $S_1^a \subset S_1$ is contracting in some sense. In particular, an impact map is quadratically stable if there exist $P_i > 0$, g_i , α_i such that

$$V_1(\Delta_1) < V_0(\Delta_0) \quad \text{for all } \Delta_0 \in S_0^d - x_0^* \quad (6)$$

Let $P > 0$ on S stand for $x'Px > 0$ for all nonzero $x \in S$. As a short hand, we will be using H_t for $H(t)$ and w_t for $w(t)$. The following theorem takes advantage of the results from section 3 to derive a set of matrix inequalities equivalent to condition (6).

Theorem 4.1 *Define*

$$R(t) = P_0 - H_t'P_1H_t - 2(g_0 - H_t'g_1)w_t + w_t'\alpha w_t$$

where $\alpha = \alpha_0 - \alpha_1$. The impact map from $\Delta_0 \in S_0^d - x_0^*$ to $\Delta_1 \in S_1^a - x_1^*$ is quadratically stable if and only if there exist $P_0, P_1 > 0$ and g_0, g_1, α such that

$$R(t) > 0 \quad \text{on } S_t - x_0^* \quad (7)$$

for all expected switching times $t \in \mathcal{T}$.

Basically, all this theorem does is substitute (2) in (6), and use both facts that the map Δ_0 to Δ_1 is linear in S_t and that, as t ranges over \mathcal{T} , S_t covers every point in S_0^d .

4.1 Approximation by a set of LMIs

There are many ways to approximate condition (7) with a set of LMIs, which can be efficiently solved using available software. By definition, condition (7) is equivalent to $\Delta_0' R(t) \Delta_0 > 0$ for all $\Delta_0 \in S_t - x_0^*$. A more conservative condition results when Δ_0 is relaxed:

$$\Delta_0' R(t) \Delta_0 > 0 \quad \text{for all } \Delta_0 \in S_0^d - x_0^*$$

If this condition is satisfied then (7) follows since $S_t \subset S_0^d$. A trivial way to obtain a set of LMIs is to further relax the constraints on Δ_0 . On one hand, this results in a more conservative condition. On the other hand, such condition is computationally more efficient.

Corollary 4.1 *The impact map from $\Delta_0 \in S_0^d - x_0^*$ to $\Delta_1 \in S_1^a - x_1^*$ is quadratically stable if there exist $P_0, P_1 > 0$ and g_0, g_1, α such that*

$$R(t) > 0 \quad \text{on } S_0 - x_0^* \tag{8}$$

for all expected switching times $t \in \mathcal{T}$.

We have then relaxed the problem of quadratic stability of impact maps to the solution of an infinite dimensional set of LMIs. As proven in several examples in sections 6 and 7, and also in [6], although condition (8) is more conservative than (7), in many situations it is enough to efficiently and successfully globally analyze PLS. In section 8, we will explain how to relax condition (7) to less conservative sets of LMIs.

Condition (8), for all $t \in \mathcal{T}$, forms an infinite set of LMIs. Computationally, to overcome this difficulty, we grid this set to obtain a finite subset of expected switching times. This grid consists of a finite sequence of equally spaced switching times $t_0 < t_1 < \dots < t_k$. In other words, $P_i > 0$, g_i , and α are found by solving a finite set of LMIs consisting of (8) on $t = \{t_i\}$, $i = 0, 1, \dots, k$. For a large enough k , it can be shown that (8) is also satisfied for all $t \in \mathcal{T}$. The idea here is to find bounds on the derivative of the minimum eigenvalue of $R(t)$ over (t_i, t_{i+1}) , and to use these bounds to show that nothing can go wrong in the intervals (t_i, t_{i+1}) , i.e., that (8) is also satisfied on each interval (t_i, t_{i+1}) (see [6] for more details).

Note that, for a given t , condition (8) reduces to a $(n-1) \times (n-1)$ LMI. This means that an increase in the dimension of the system only results in proportionally larger LMIs. Thus, the stability condition (8) scales with the dimension of the system.

4.2 Proof of Results

Proof of theorem 4.1: From (6) and using theorem 3.1, we have

$$\begin{aligned} & \Delta_1' P_1 \Delta_1 - 2\Delta_1' g_1 + \alpha_1 < \Delta_0' P_0 \Delta_0 - 2\Delta_0' g_0 + \alpha_0 \\ \Leftrightarrow & \Delta_0' H_t' P_1 H_t \Delta_0 - 2\Delta_0' H_t' g_1 + \alpha_1 < \Delta_0' P_0 \Delta_0 - 2\Delta_0' g_0 + \alpha_0 \\ \Leftrightarrow & \Delta_0' (P_0 - H_t' P_1 H_t) \Delta_0 - 2\Delta_0' (g_0 - H_t' g_1) + \alpha > 0 \end{aligned}$$

Finally, using (4) we have

$$\Delta_0' (P_0 - H_t' P_1 H_t) \Delta_0 - 2\Delta_0' (g_0 - H_t' g_1) w_t \Delta_0 + \Delta_0' w_t' \alpha w_t \Delta_0 > 0$$

Condition (7) follows from corollary 3.1, which proofs the desired result. ■

Proof of corollary 4.1: The result follows since $S_t \subset S_0$. ■

5 Global Analysis of PLS

The previous section explained how a single impact map can be globally analyzed using SuLF. For some PLS, like some relay feedback systems, the analysis of a single impact map is all it takes to globally analyze the system [6]. However, that is not enough for most PLS. In general, it is required that multiple impact maps are simultaneously quadratically stable. This section briefly explains the three main steps to achieve this goal (the details are left to sections 6 and 7). These are: (1) characterization of impact maps; (2) definition of quadratic Lyapunov functions at switching surfaces; and (3) solution of stability conditions. In more detail:

Step 1: *Impact Maps*

1. Identification of all impact maps associated with the PLS. If the system has m switching surfaces then there are at the most $2m^2$ impact maps. The actual number of impact maps required to analyze the system is typically smaller due to certain properties of a system, like symmetry (see relay feedback systems [6] or saturation systems (section 7) or just the fact that not all switches are possible.
2. Domain of impact maps. In order to reduce conservatism, it is important to characterize the domain of each impact map, as explained in section 8.1. Impact maps that have an empty domain set do not need to be further considered, neither those points in a switching surface that converge asymptotically to the origin without switching (see the middle of figure 3).
3. Expected switching times. For each impact map find the set of expected switching times \mathcal{T} .
4. Switching conditions. Certain necessary conditions need to be checked in order to guarantee that a trajectory, starting in a switching surface, does not grow unbounded without switching (as in the left of figure 3).
5. Linear decomposition. For each impact map, we need to find an x_0^* belonging to the switching surface where the domain of an impact is defined, such that the assumption of theorem 3.1 is satisfied. If this is not possible, the switching times where the assumption is not satisfied need to be characterized, and then proceed as explained in section 3.

Step 2: *Quadratic Surface Lyapunov Functions (SuLF)*

1. Define all SuLF on the respective domains of impact maps. There are at the most $2m$ SuLF, where m is the number of switching surfaces of the PLS. This number can be smaller depending if the system has certain symmetric properties.
2. Constraints on SuLF: continuity issues, and limit cycles and equilibrium points. When the domain of two impact maps share a common boundary on some switching surface, in that boundary both impact maps have zero switching time. That implies that the Lyapunov functions defined on those domains must be continuous along that boundary. Also, if a limit cycle intersects the domain of an impact map or an equilibrium point belongs to that domain, then the associated Lyapunov function must be a quadratic form, i.e., $g_i = 0$ and $\alpha_i = 0$ in (5).

Step 3: *Stability Conditions*

1. For each impact map, theorem 4.1 provides a quadratic inequality that must be satisfied for all expected switching times \mathcal{T} associated with the impact map. Corollary 4.1 can be used to write the stability conditions as LMIs, which can be solved for the parameters of the SuLF.
2. Bounds on expected switching times. In many situations it is not necessary to check if a quadratic inequality associated with an impact map is satisfied for all expected switching times $t \in \mathcal{T}$, but it is enough to check if this is satisfied a bounded subset of \mathcal{T} .
3. Improvement of stability conditions. If the LMIs provided by corollary 4.1 fail to find a not feasible solution then we can use less conservative conditions, as explained in section 8.
4. An alternative to solving all the LMIs described above is to add LMIs until all quadratic constraints are satisfied. Since checking if a quadratic inequality is satisfied is much easier than solving the correspondent LMIs, the following algorithm can be used:
 - (a) Initialize the SuLF with some parameters. The set of LMIs is an empty set at this time.
 - (b) Check if all quadratic inequalities are satisfied for all expected switching times bounds.
 - (c) If not, take a quadratic inequality that was not satisfied for some switching time bound, and add it to the set of LMIs. Solve the set of LMIs, get new parameters for the SuLF, and go back to (b).
 - (d) If yes, the algorithm ends.

Before attempting to use this algorithm to analyze general classes of PLS, it is important to fully understand in detail each of the steps in the algorithm. For that purpose, we have analyzed several classes of PLS by increasing order of complexity. Each of these classes was carefully chosen to (1) separately deal with different issues in each step of the algorithm and (2) to illustrate with examples the efficiency of this new methodology. By increasing complexity, we first analyzed relay feedback systems [6], then on/off systems (section 6), and finally saturation systems (section 7). The success in globally analyzing a large number of examples of these classes of PLS demonstrated the potential of these new ideas in globally analyzing other, more complex classes of PLS.

The reasons for analyzing these particular classes of PLS are the following. In relay feedback systems [6], we analyzed limit cycles. The choice to first analyze this class of PLS was based on the fact that, for symmetric unimodal limit cycles, there is only a single impact map that needs to be studied. This means that global analysis of symmetric unimodal limit cycles of relay feedback systems follows directly from theorem 4.1.

In section 6, we analyze on/off systems to explain (1) how this new methodology is used to globally analyze equilibrium points and (2) how more than one impact map is simultaneously analyzed. Then, with saturation systems (section 7) we show how to deal with multiple switching surfaces. Analysis of other, more complex classes of PLS can be done using a combination of the ideas discussed above.

6 On/Off Systems

This section addresses the problem of global stability analysis of *on/off systems* (OFS) SuLF, showing that this tool can be used to prove global asymptotic stability of equilibrium points of PLS.

The ideas introduced in sections 3 and 4 were very successful in proving global asymptotic stability of symmetric unimodal limit cycles of RFS [6]. In this case, there was only a single impact map that needed to be analyzed due to the symmetry of RFS. In this section, we show that SuLF can also be used to efficiently prove global asymptotic stability of equilibrium points, even when these equilibrium points do not belong to the switching surface.

To demonstrate these ideas, we chose a class of PLS known as on/off systems (OFS). An OFS can be thought of as an LTI system that switches between open and closed loop. The switches are determined by the values of the output of the LTI system. OFS can be found in many engineering applications. In electronic circuits, diodes can be approximated by on/off nonlinearities. Also, transient behavior of logical circuits that involve latches/flip-flops performing on/off switching can be modeled with on/off circuits and saturations. Another area of application of OFS is aircraft control. For instance, in [2], a *max* controller is designed to achieve good tracking of the pilot's input without violating safety margins.

We are interested in checking if a unique locally stable equilibrium point of an OFS is globally asymptotically stable. The idea is to construct quadratic Lyapunov functions on the switching surface of the system to show contraction in some sense of impact maps. Under certain easily verifiable conditions, quadratic stability of impact maps implies globally asymptotic stability of OFS. The search for quadratic surface Lyapunov functions is efficiently done by solving a set of LMIs.

As in relay feedback systems, a large number of examples was successfully proven globally stable. These include systems with an unstable affine linear subsystem, systems of relative degree larger than one and of high dimension, and systems with unstable nonlinearity sectors, for which classical methods like small gain theorem, Popov criterion, Zames-Falb criterion [20], and integral quadratic constraints [3, 10, 12, 13], fail to analyze. In fact, it is still an open problem whether there exists an example with a globally stable equilibrium point that could not be successfully analyzed with this new methodology.

6.1 Problem Formulation

We start by defining OFS followed by some necessary conditions for the global stability of a unique locally stable equilibrium point. We then talk about some of the properties of this class of systems.

An OFS is defined as follows. Consider a SISO LTI system satisfying the following linear dynamic equations

$$\begin{cases} \dot{x} &= Ax + Bu \\ y &= Cx \end{cases} \quad (9)$$

where $x \in \mathbb{R}^n$, in feedback with a on/off controller (see figure 7) given by

$$u(t) = \max \{0, y(t) - d\} \quad (10)$$

where $d \in \mathbb{R}$. By a solution of (9)-(10) we mean functions (x, y, u) satisfying (9)-(10). Since u is continuous and globally Lipschitz, $Ax + B \max \{0, Cx - d\}$ is also globally Lipschitz. Thus, the OFS has a unique solution for any initial state.

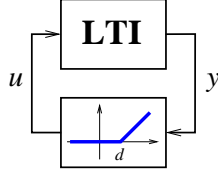


Figure 7: On/off system

In the state space, the on/off controller introduces a switching surface composed of an hyperplane of dimension $n - 1$ given by

$$S = \{x \in \mathbb{R}^n : Cx = d\}$$

On one side of the switching surface ($Cx < d$), the system is given by $\dot{x} = Ax$. On the other side ($Cx > d$) the system is given by $\dot{x} = Ax + B(Cx - d) = A_1x + B_1$, where $A_1 = A + BC$ and $B_1 = -Bd$. Note that the vector field is continuous along the switching surface since for any $x \in S$, $A_1x + B_1 = Ax$.

An OFS has either zero, one, two, or a continuum of nonisolated equilibrium points. We are interested in those cases where the system has a unique locally stable equilibrium point. Only here can an OFS have a globally stable equilibrium point. Next, we give necessary conditions for the existence of a single locally stable equilibrium point for different values of d .

If $d > 0$ there is at least one equilibrium point at the origin. In this case, it is necessary that A is Hurwitz to guarantee the origin is locally stable. If A_1 is invertible, the affine linear system $\dot{x} = A_1x + B_1$ has an equilibrium point at $-A_1^{-1}B_1$. In order to guarantee the OFS has only the origin as an equilibrium point, it is necessary that $-CA_1^{-1}B_1 < d$. It is also necessary that A_1 has no real unstable eigenvalues or, otherwise, the system will have trajectories that grow unbounded⁴.

When $d = 0$, the origin is the only equilibrium point. For the same reasons as above, it is necessary that both A and A_1 do not have real unstable eigenvalues. Note that in this case, there is no “easy” way to check if the origin is locally stable or not.

When $d < 0$, it must be true that A_1 is Hurwitz and A has no real unstable poles. It is also necessary that $-CA_1^{-1}B_1 > d$ or otherwise the system will have no equilibrium point.

We can assume without loss of generality that $d \geq 0$. If $d < 0$ and all necessary conditions are met, with an appropriate change of variables ($x_{new} = -(x + A_1^{-1}B_1)$), the problem can be transformed to one of analyzing the origin with $d_{new} \geq 0$. In this case, $A_{new} = A_1$, $A_{1new} = A$, $B_{1new} = AA_1^{-1}B_1$, and $d_{new} = -d - CA_1^{-1}B_1 \geq 0$.

Consider a subset S_+ of S given by

$$S_+ = \{x \in S : CAx \geq 0\}$$

This set is important since it tells us which points in S can be reached by trajectories starting at any x_0 such that $Cx_0 < d$ (see the left of figure 8). Similarly, define $S_- \subset S$ as $S_- = \{x \in S : CAx \leq 0\}$. Note that $S = S_+ \cup S_-$ and $S_+ \cap S_- = \{x \in S : CAx = 0\}$. From here on, we assume $d > 0$. In terms of stability analysis, $d = 0$ is a special case of when $d > 0$, and will be considered separately in section 6.5.

⁴Possible exceptions occur when the eigenvector associated with the unstable real eigenvalue is perpendicular to C .

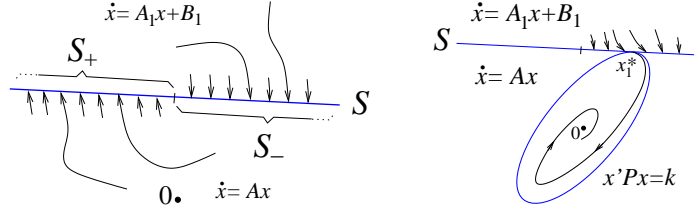


Figure 8: Both sets S_+ and S_- in S (left); how to obtain x_1^* (right)

Since A must be Hurwitz, there is a set of points in S_- such that any trajectory starting in that set will never switch again and will converge asymptotically to the origin. In other words, let $S^* \subset S_-$ be the set of points x_0 such that $Ce^{At}x_0 = d$ does not have a solution for any $t > 0$. Note that this set S^* is not empty. To see this, let $P > 0$ satisfy $PA + A'P = -I$. Then, an obvious point in S^* is the point x_1^* obtained from the intersection of S with the level set $x'Px = k$, where $k \geq 0$ is chosen such that the ellipse $x'Px = k$ is tangent to S (see the right side of figure 8).

6.2 Impact maps for on/off systems

The problem we propose to solve here is to give sufficient conditions that, when satisfied, prove the origin of an OFS is globally asymptotically stable. The strategy of this proof is as follows. Consider a trajectory starting at some point $x_0 \in S_+$ (see figure 9). If all necessary conditions are met, the trajectory $x(t)$ will eventually switch at some time $t_1 > 0$, i.e., $Cx(t_1) = d$ and $Cx(t) \geq d$ for $t \in [0, t_1]$. Let $x_1 = x(t_1) \in S_-$. If $x_1 \in S^*$, the trajectory will not switch again and converges asymptotically to the origin. Since we already know S^* is a stable set, we need to concentrate on those points in $S_- \setminus S^*$ since those are the ones that may lead to potentially unstable trajectories. So, assume the trajectory switches again at time $t_2 > t_1$, and let $x_2 = x(t_2) \in S_+$. Again, we would switch at $x_3 = x(t_3)$ and so on. The idea is to check if x_3 is closer in some sense to S^* than x_1 . If so, this would mean that eventually $x(t_{2N-1}) \in S^*$, for some large enough positive integer N , and prove that the origin is globally asymptotically stable. This is the basic idea behind the results in the next subsection.

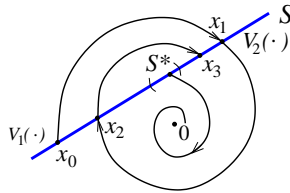


Figure 9: Trajectory of an OFS

It is convenient to notice that $x_0, x_1, x_2 \in S$ can be parametrized. Let $x_0 = x_0^* + \Delta_0$, $x_1 = x_1^* + \Delta_1$, and $x_2 = x_2^* + \Delta_2$, where $x_0^*, x_1^* \in S$, and $C\Delta_0 = C\Delta_1 = C\Delta_2 = 0$. Also, define $x_0^*(t)$ ($x_1^*(t)$) as the trajectory of $\dot{x} = A_1x + B_1$ ($\dot{x} = Ax$), starting at x_0^* (x_1^*), for all $t \geq 0$. Since x_i^* can be any points in S , we chose them to be such that $Cx_i^*(t) < d$ for all $t > 0$. As explained in appendix A.1, this is always possible, even when A_1 is unstable (as long as it has at least one stable eigenvalue with an associated eigenvector that is not perpendicular to C'). The reason for this particular choice of x_0^* and x_1^* is so that $Cx_i^*(t) - d \neq 0$ for all $t > 0$. This will be necessary in proposition 6.1.

There are two impact maps of interest associated with an OFS. The first impact map—impact map 1—takes points from S_+ (the departure set of impact map 1) and maps them in S_- (the associated arrival set). The second impact map—impact map 2—takes points from $S_- \setminus S^*$ (the departure set of impact map 2) and maps them back to S_+ (the associated arrival set). Note that S^* does not belong to the domain of either impact map since every trajectory starting in S^* does not switch again.

As in RFS [6], the impact maps associated with OFS are, in general, multivalued. Define the sets of expected switching times \mathcal{T}_1 and \mathcal{T}_2 as the sets of all possible switching times associated with each respective impact map (see definition 3.1). Define also $S_{t_1} \subset S_+$ and $S_{t_2} \subset S_- \setminus S^*$ similarly as S_t was defined in section 3. Considering first impact map 1, for each point $x_0 \in S_+$ there is an associated switching time t_1 . For each $t_1 \in \mathcal{T}_1$, define S_{t_1} as the set of all initial conditions $x_0 \in S_+$ such that $Cx(t) \geq d$ on $[0, t_1]$, and $Cx(t_1) = d$. Thus, S_{t_1} is the set of points in S_+ that have an associated switching time t_1 . Analogously, for each $t_2 \in \mathcal{T}_2$ define S_{t_2} for impact map 2 as the set of all initial conditions $x_1 \in S_- \setminus S^*$ such that $y(t) \leq d$ on $[0, t_2]$, and $y(t_2) = d$. Note that both S_{t_1} and S_{t_2} are subsets of linear manifolds of dimension $n - 2$.

6.3 Global asymptotic stability of on/off systems

Before presenting the main result of this section, we use theorem 3.1 to show that each impact map associated with an OFS can be represented as a linear transformation analytically parametrized by the correspondent switching time.

Proposition 6.1 *Define*

$$w_1(t) = \frac{Ce^{A_1 t}}{d - Cx_0^*(t)} \quad \text{and} \quad w_2(t) = \frac{Ce^{At}}{d - Cx_1^*(t)}$$

Let $H_1(t) = e^{A_1 t} + (x_0^*(t) - x_1^*)w_1(t)$ and $H_2(t) = e^{At} + (x_1^*(t) - x_0^*)w_2(t)$. Then, for any $\Delta_0 \in S_+ - x_0^*$ there exists a $t_1 \in \mathcal{T}_1$ such that $\Delta_1 = H_1(t_1)\Delta_0$. Such t_1 is the switching time associated with Δ_1 . Similarly, for any $\Delta_1 \in S_- \setminus S^* - x_1^*$ there exists a $t_2 \in \mathcal{T}_2$ such that $\Delta_2 = H_2(t_2)\Delta_1$. Such t_2 is the switching time associated with Δ_2 .

Next, define two quadratic Lyapunov functions V_1 and V_2 on the switching surface S

$$V_i(x) = x'P_i x - 2x'g_i + \alpha_i \quad (11)$$

where $P_i > 0$, for $i = 1, 2$. Global asymptotically stability of the origin follows if both impact maps are simultaneously quadratically stable, i.e., if there exist $P_i > 0$, g_i , α_i such that

$$V_2(\Delta_1) < V_1(\Delta_0) \quad \text{for all } \Delta_0 \in S_+ - x_0^* \quad (12)$$

$$V_1(\Delta_2) < V_2(\Delta_1) \quad \text{for all } \Delta_1 \in S_- \setminus S^* - x_1^* \quad (13)$$

The next theorem is an extension of theorem 4.1 for the case where we have to simultaneously prove contraction of two impact maps. As a short hand, in the following result we use $H_{it} = H_i(t)$ and $w_{it} = w_i(t)$.

Theorem 6.1 *Define*

$$\begin{aligned} R_1(t) &= P_1 - H'_{1t}P_2H_{1t} - 2(g_1 - H'_{1t}g_2)w_{1t} + w'_{1t}\alpha w_{1t} \\ R_2(t) &= P_2 - H'_{2t}P_1H_{2t} - 2(g_2 - H'_{2t}g_1)w_{2t} - w'_{2t}\alpha w_{2t} \end{aligned}$$

where $\alpha = \alpha_1 - \alpha_2$. The origin of the OFS is globally asymptotically stable if there exist $P_1, P_2 > 0$ and g_1, g_2, α such that

$$\begin{cases} R_1(t_1) > 0 & \text{on } S_{t_1} - x_0^* \\ R_2(t_2) > 0 & \text{on } S_{t_2} - x_1^* \end{cases} \quad (14)$$

for all expected switching times $t_1 \in \mathcal{T}_1$ and $t_2 \in \mathcal{T}_2$.

As in corollary 4.1, a relaxation of the constraints on Δ_0 and Δ_1 in the previous theorem results in computationally efficient conditions.

Corollary 6.1 *The origin of the OFS is globally asymptotically stable if there exist $P_1, P_2 > 0$ and g_1, g_2, α such that*

$$\begin{cases} R_1(t_1) > 0 & \text{on } S - x_0^* \\ R_2(t_2) > 0 & \text{on } S - x_1^* \end{cases} \quad (15)$$

for all expected switching times $t_1 \in \mathcal{T}_1$ and $t_2 \in \mathcal{T}_2$.

For each t_1, t_2 these conditions are LMIs for which we can solve for $P_1, P_2 > 0$ and g_1, g_2, α using efficient available software. As we will see in the next section, although these conditions are more conservative than the ones in theorem 6.1, they are already enough to prove global asymptotic stability of many important OFS.

Each condition in (15) depends only on a single scalar parameter, i.e., R_1 depends only on t_1 and not on t_2 , and, similarly, R_2 depends only on t_2 . Computationally, this means that when we grid each set of expected switching times, this will only affect one of the conditions in (15). Thus, if we need m_1 samples of \mathcal{T}_1 and m_2 samples of \mathcal{T}_2 , we end up with a total of $m_1 + m_2$ LMIs. Note that a less conservative condition than those in theorem 6.1 could be obtained. Such condition, of the form $R(t_1, t_2) > 0$, would, however, lead to $m_1 \times m_2$ LMIs, and the analysis problem would easily become computationally intractable. This difference in complexity is even more obvious in the analysis of other, more complex classes of PLS that may require the simultaneous analysis of a large number of impact maps.

As explained in section 4.1, it is possible to make conditions (14) less conservative at a cost of increase computations. In section 8, and, in particular, section 8.3, we will explain how to approximate conditions (14) with less conservative sets of LMIs than (15).

6.4 Examples

The following examples were processed in `matlab` code. The latest version of this software is available at [7]. Before presenting the examples, we briefly explain the `matlab` function we developed. The inputs to this function are a transfer function of an LTI system together with the displacement of the nonlinearity switch d . If the OFS is proven to be globally stable, the function returns the values of the parameters of the Lyapunov functions (11). The `matlab` function also returns a graphic showing the minimum eigenvalues of each $R_i(t_i)$ in (15), which must be positive for all expected switching times t_i .

For most OFS, the expected switching times include $t_i = 0$ and large values of t_i . Thus, before moving into the examples, it is important to explain how the analysis is done when t_i is close to zero and when t_i is large. We start with the analysis near zero.

Zero switching time corresponds to points in S such that $CAx = 0$. At those points, the Lyapunov functions (11) must be continuous since this is the only way both $V_2(\Delta_1) \leq V_1(\Delta_0)$ and $V_1(\Delta_2) \leq V_2(\Delta_1)$ can be simultaneously satisfied, for all $\Delta_0, \Delta_1, \Delta_2 = \Delta_0$ such that $x_0^* + \Delta_0 = x_1^* + \Delta_1$ and $CA(x_0^* + \Delta_0) = 0$. Therefore, we need $V_1(\Delta_0) = V_2(\Delta_1)$. This imposes certain restrictions on $P_1, P_2 > 0$, g_1, g_2 , and α . The details can be found in appendix A.2.

Just like in RFS [6], we would like to obtain bounds on the expected switching times. With the exception of 3^{rd} -order systems, however, finding upper bounds t_{imax} on switching times is, in general, not an easy task. The idea is to first guarantee conditions (15) are satisfied in some intervals $(0, t_{imax})$ and then check if they are also valid for all $t_i > t_{imax}$. This is considered in appendix A.3. Note that the limits of $R_1(t)$ and $R_2(t)$ as $t \rightarrow \infty$ are equal to P_1 and P_2 , respectively. Thus, it is guaranteed that (14) and (15) are satisfied at $t = \infty$ since both $P_1 > 0$ and $P_2 > 0$.

Example 6.1 Consider the OFS on the left of figure 10 with $d = 1$. It is easy to see that the origin of this system is locally stable.

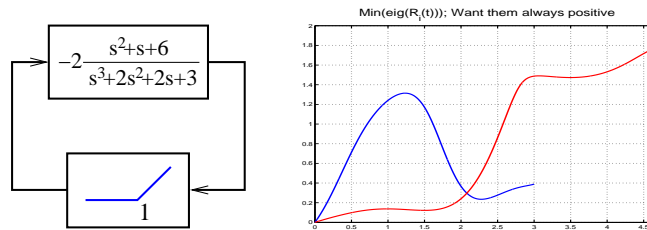


Figure 10: 3^{rd} -order system with unstable nonlinearity sector

Using conditions (15), we show that the origin is in fact globally asymptotically stable. The right side of figure 10 illustrates this fact: the minimum eigenvalue of each condition (15) is positive on its respective set of expected switching times. The expected switching times in this example are approximately $\mathcal{T}_1 = (0, 1.85)$ and $\mathcal{T}_2 = (0, 4.7)$. For instance, if $t_1 \geq 1.85$, there is no point in S_+ with switching time equal to t_1 .

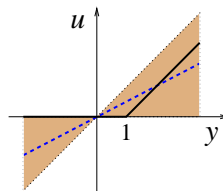


Figure 11: On/off controller versus constant gain of $1/2$ (dashed)

Note that this system has an unstable nonlinearity sector. If the on/off nonlinearity is replaced by a linear constant gain of $1/2$, the system becomes unstable (see figure 11). This is very interesting since it tells us that analysis tools like small gain theorem, Popov criterion, Zames–Falb criterion, and integral quadratic constraints, would all fail to analyze OFS of this nature. ■

Example 6.2 Consider the OFS on the left of figure 12 with $d = 1$ and $k > 0$. Once again, it is easy to see that the origin of this system is locally stable for any $k > 0$.

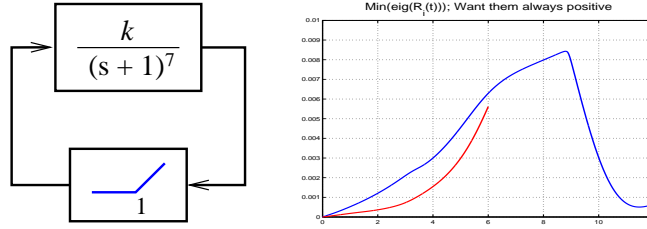


Figure 12: System with relative degree 7 (left); global stability analysis for $k = 2$ (right)

Note that $\|Ce^{At}B\|_{\mathcal{L}_1} = k$. Thus, the small gain theorem can be applied whenever $k \leq 1$. When $k > 1$, however, the small gain theorem fails to analyze the system.

Let $k = 2$. Using conditions (15), we show the origin is globally asymptotically stable. The right side of figure 12 shows how conditions (15) are satisfied in some intervals $(0, t_{imax})$, $i = 1, 2$. The intervals $(0, t_{imax})$ are bounds on the expected switching times. The results in appendix A.3 guarantee the stability conditions are also satisfied for all $t_i > t_{imax}$. For details on how to find such bounds see appendix A.3. ■

Example 6.3 Consider the OFS in figure 13 with $d = 1$. It is easy to see that the origin of this system is locally stable. A_1 , however, is unstable.

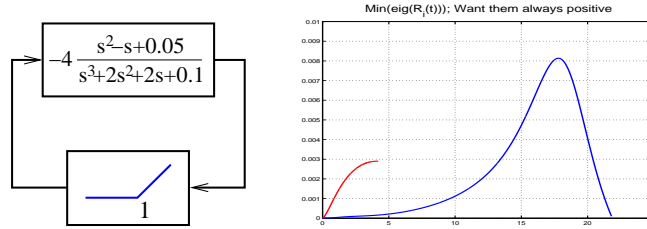


Figure 13: System with unstable A_1

Although A_1 is unstable, since this is a 3^{rd} -order system, it is easy to find bounds on the expected switching times for the subsystem $\dot{x} = A_1x + B_1$ due to the fact that the switching surface is an hyperplane of dimension 2, which can be visualized. In this case, no point in S_+ has a switching time larger than 21.8. As for t_2 , we use the same ideas as in the previous example, based on the results in appendix A.3. Using conditions (15), we show that although A_1 is unstable, the origin is globally asymptotically stable. The right side of figure 13 shows how conditions (15) are satisfied in the intervals $(0, t_{imax})$, $i = 1, 2$ (the minimum eigenvalue of the second condition in (15) is scaled by 500 in figure 13, for purpose of visualization). ■

6.5 Special case: $d = 0$

When $d = 0$ we can write stability conditions in the form of LMIs that are, in general, much less conservative than conditions (15) and even conditions (30). First, since the origin belongs to both systems $\dot{x} = Ax$ and $\dot{x} = (A + BC)x$, it is only required that both systems do not have real unstable poles. $d = 0$ also means $x_0^* = x_1^* = g_1 = g_2 = 0$ and $\alpha = 0$. All we need to find is $P_1, P_2 > 0$.

In this case, $\Delta_1 = e^{A_1 t_1} \Delta_0$ and $\Delta_2 = e^{A_2 t_2} \Delta_1$. Thus, the stability conditions are simply

$$\begin{cases} \Delta'_1 P_2 \Delta_1 < \Delta'_0 P_1 \Delta_0 \\ \Delta'_2 P_1 \Delta_2 < \Delta'_1 P_2 \Delta_1 \end{cases} \Leftrightarrow \begin{cases} \Delta'_0 \left(P_1 - e^{A_1 t_1} P_2 e^{A_1 t_1} \right) \Delta_0 > 0 \\ \Delta'_1 \left(P_2 - e^{A_2 t_2} P_1 e^{A_2 t_2} \right) \Delta_1 > 0 \end{cases}$$

for some $P_1, P_2 > 0$, all $\Delta_0 \in S_{t_1}$, $\Delta_1 \in S_{t_2}$, and all expected switching times t_1, t_2 .

Notice that $C\Delta_0 = 0$, $C\Delta_1 = 0$, and $C\Delta_2 = 0$. Thus, $Ce^{A_1 t_1} \Delta_0 = 0$ and $Ce^{A_2 t_2} \Delta_1 = 0$. That is, for fixed values of t_1 and t_2 , Δ_1 and Δ_2 are restricted to a subspace of dimension $n - 2$. Let $\Pi \in C^\perp$, where C^\perp are the *orthogonal complements* to C , i.e., matrices with a maximal number of column vectors forming an orthonormal set such that $CC^\perp = 0$. Let also $l_{t_1} \in (Ce^{A_1 t_1} \Pi)^\perp$ and $l_{t_2} \in (Ce^{A_2 t_2} \Pi)^\perp$. We have the following result.

Theorem 6.2 *The origin of the OFS with $d = 0$ is globally asymptotically stable if there exist $P_1, P_2 > 0$ such that*

$$\begin{cases} l'_{t_1} \Pi' \left(P_1 - e^{A_1 t_1} P_2 e^{A_1 t_1} \right) \Pi l_{t_1} > 0 \\ l'_{t_2} \Pi' \left(P_2 - e^{A_2 t_2} P_1 e^{A_2 t_2} \right) \Pi l_{t_2} > 0 \end{cases} \quad (16)$$

for all expected switching times $t_1 \in \mathcal{T}_1$ and $t_2 \in \mathcal{T}_2$.

7 Saturation Systems

The state space of on/off systems was divided in two partitions by a single switching surface. In this section, we show how impact maps and SuLF can also be used to globally analyze PLS with more than two state-space partitions and more than one switching surface.

To demonstrate these ideas, we chose a class of PLS known as *saturation systems* (SAT). The class of SAT we consider consists of an LTI system in feedback with a saturation. The study of such systems is motivated by the possibility of actuator saturation or constraints on the actuators, reflected sometimes in bounds on available power supply or rate limits. Because feedback is cut, control saturation induces a nonlinear behavior on the closed-loop system that cannot be naturally dealt within the context of standard (algebraic) linear control theory. It is well known that linear feedback laws when saturated can lead to instability. Thus, the problem of stabilizing linear systems with bounded controls has been extensively studied. See, for example, [16, 18, 19] and references therein.

In terms of analysis, there exist several results for SAT. The Popov criterion can be used as a simplified approach to the analysis, but it is expected to be very conservative for systems of order greater than three. The Zames–Falb criterion [20] can be used when the nonlinearity's slope is restricted, like in this case, but the method is difficult to implement. IQC-based analysis [3, 10, 12, 13] gives conditions in the form of LMIs that, when satisfied, guarantee stability of SAT. However, none of these analysis tools can be used when a SAT has an unstable nonlinearity sector.

Here, we propose to construct SuLF for SAT to show that impact maps associated with the system are contracting in some sense. This, in turn, proves the origin of a SAT is globally asymptotically stable. As in the case of on/off systems, a large number of examples was successfully proven globally stable. These include high-order systems, systems of relative degree larger than one, and systems with unstable nonlinearity sectors for which all classical methods fail to analyze. In fact, existence of an example with a globally stable equilibrium point that could not be successfully analyzed with this new methodology is still an open problem.

7.1 Problem Formulation

We start by defining a saturation system (SAT) followed by some necessary conditions for global stability of a unique locally stable equilibrium point. We then talk about some of the properties of this class of PLS.

Consider a SISO LTI system (9) in feedback with a saturation controller (see figure 14) defined as

$$u(t) = \begin{cases} -d & \text{if } y(t) < -d \\ y(t) & \text{if } |y(t)| \leq d \\ d & \text{if } y(t) > d \end{cases} \quad (17)$$

where $d > 0$ (if $d = 0$ then the system is simply linear). By a solution of (9),(17) we mean functions (x, y, u) satisfying (9),(17). Since u is continuous and globally Lipschitz, $Ax + Bu$ is also globally Lipschitz. Thus, the SAT has a unique solution for any initial state.

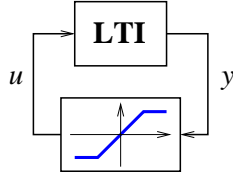


Figure 14: Saturation system

In the state space, the saturation controller introduces two switching surfaces composed of hyperplanes of dimension $n - 1$ given by

$$S = \{x \in \mathbb{R}^n : Cx = d\}$$

and

$$\underline{S} = -S = \{x \in \mathbb{R}^n : Cx = -d\}$$

On one side of the switching surface S ($Cx > d$), the system is governed by $\dot{x} = Ax + Bd$. In between the two switching surfaces ($|Cx| \leq d$), the system is given by $\dot{x} = Ax + BCx = A_1x$, where $A_1 = A + BC$. Finally, on the other side of \underline{S} ($Cx < -d$) the system is governed by $\dot{x} = Ax - Bd$. Note that the vector field (9),(17) is continuous along the switching surfaces since, for any $x \in S$, $A_1x = (A + BC)x = Ax + Bd$, and for any $x \in \underline{S}$, $A_1x = Ax - Bd$.

SAT can exhibit extremely complex behaviors. Some SAT may be chaotic, others may have one, three, or a continuum of equilibrium points, or limit cycles, or even some combination of all these behaviors. We are interested in those SAT with a unique locally stable equilibrium point. Only here can a SAT be globally stable. For that, it is necessary that $A + BC$ is Hurwitz in order to guarantee the origin is locally stable, and, if A is invertible, that $-CA^{-1}B < 1$, so the origin is the only equilibrium point. It is also necessary that A has no eigenvalues with positive real part, or otherwise there are initial conditions for which the system will grow unbounded (see, for example, [17]).

Consider a subset S_+ of S given by

$$S_+ = \{x \in S : CA_1x \geq 0\}$$

As in OFS, this set tells us which points in S correspond to the first switch of trajectories starting at any x_0 such that $Cx_0 < d$. In other words, S_+ is the set of points in S that can be reached by trajectories of (9),(17) when governed by the subsystem $\dot{x} = A_1x$. In a similar way, define $S_- \subset S$ as $S_- = \{x \in S : CA_1x \leq 0\}$ and also $\underline{S}_+ = -S_+$ and $\underline{S}_- = -S_-$.

As in OFS, since A_1 must be Hurwitz, there is a set of points in S_- such that any trajectory starting in that set will not switch again and will converge asymptotically to the origin. In other words, let $S^* \subset S_-$ be the set of points x_0 such that $Ce^{A_1 t}x_0 = \pm d$ do not have a solution for any $t > 0$. Note that this set S^* is not empty. To see this, let $P > 0$ satisfy $PA_1 + A_1'P = -I$. Then, an obvious point in S^* is the point x_1^* obtained from the intersection of S with the level set $x'Px = k$, where $k \geq 0$ is chosen such that the ellipse $x'Px = k$ is tangent to both S and \underline{S} .

7.2 Impact maps for saturation systems

The problem we propose to solve is to give sufficient conditions that, when satisfied, prove the origin of a SAT is globally asymptotically stable. The strategy of the proof is similar to OFS. The main difference is that a trajectory starting at some point $x_1 \in S_- \setminus S^*$ can either switch at some point in S or switch at some point in \underline{S} (see figure 15). Let $S_d \subset (S_- \setminus S^*)$ ($S_{-d} \subset (\underline{S}_- \setminus S^*)$) be the set of points that will switch in S (\underline{S}). If $x_1 \in S_d$ ($x_1 \in S_{-d}$) the trajectory switches in finite time t_{2a} (t_{2b}) at $x_{2a} = x(t_{2a}) \in S_+$ ($x_{2b} = x(t_{2b}) \in \underline{S}_+$). Then, it would switch again at $x_{3a} = x(t_{3a})$ ($x_{3b} = x(t_{3b})$), and so on. As in section 6, the idea is to check if x_{3a} or $-x_{3b}$ are closer in some sense to S^* than x_1 . If so, this would mean that eventually $x(t_N) \in S^*$, for some large enough N , and prove that the origin is globally asymptotically stable.

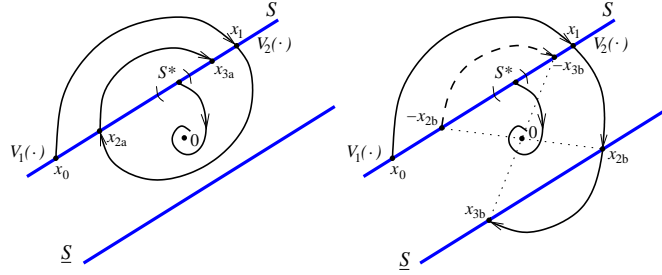


Figure 15: Possible state-space trajectories for a SAT

Since $x_0, x_1, x_{2a} \in S$ and $x_{2b} \in \underline{S}$, we can write $x_0 = x_0^* + \Delta_0$, $x_1 = x_1^* + \Delta_1$, $x_{2a} = x_0^* + \Delta_{2a}$ and $x_{2b} = -x_0^* + \Delta_{2b}$, where $x_0^*, x_1^* \in S$ and $C\Delta_0 = C\Delta_1 = C\Delta_{2a} = C\Delta_{2b} = 0$. Also, define $x_0^*(t)$ ($x_1^*(t)$) as the trajectory of $\dot{x} = Ax + Bd$ ($\dot{x} = A_1x$), starting at x_0^* (x_1^*), for all $t \geq 0$. Since x_i^* are any points in S , we chose them to be such that $Cx_i^*(t) < d$ for all $t > 0$. The reason for this particular choice of x_0^* and x_1^* is so that $Cx_i^*(t) - d \neq 0$ for all $t > 0$. This choice of x_0^* and x_1^* is always possible. x_1^* is found as explained above. In this case, $x_1^* \in S^*$ is given by

$$x_1^* = \frac{P_d^{-1}C'}{CP_d^{-1}C'}d$$

where $P_d > 0$ satisfies $P_dA_1 + A_1'P_d = -I$. In a similar way, whenever A is a stable matrix, x_0^* is given by

$$x_0^* = (d + cA^{-1}Bd) \frac{P_u^{-1}C'}{CP_u^{-1}C'} - A^{-1}Bd$$

where $P_u > 0$ satisfies $P_uA + A'P_u = -I$. If A is not stable, x_0^* is found as in appendix A.1.

Just like RFS, a property of SAT is their symmetry around the origin. Thus, for analysis purposes, it is equivalent to consider the trajectory starting at x_{2b} or $-x_{2b}$ (see figure 15). This means that the impact maps of interest associated with a SAT reduce to only three.

The first impact map (impact map 1) takes points from S_+ and maps them in S_- . The second impact map (impact map 2a) takes points from $S_d \subset S_-$ and maps them back to S_+ . Finally, the third impact map (impact map 2b) takes points from $S_{-d} \subset S_-$ and maps them in \underline{S}_+ . As in RFS and OFS, the impact maps associated with SAT are, in general, multivalued. Define the sets of expected switching times \mathcal{T}_1 , \mathcal{T}_{2a} , and \mathcal{T}_{2b} as the sets of all possible switching times associated with each respective impact map. In appendix B, we show how to obtain bounds on these sets. Define also S_{t_1} , $S_{t_{2a}}$, and $S_{t_{2b}}$ as in section 3 and 6.2.

7.3 Global asymptotic stability of saturation systems

The linear representation of impact maps associated with SAT follows as in theorem 3.1 and OFS.

Proposition 7.1 *Define*

$$w_1(t) = \frac{Ce^{At}}{d - Cx_0^*(t)}, \quad w_{2a}(t) = \frac{Ce^{A_1t}}{d - Cx_1^*(t)}, \quad w_{2b}(t) = \frac{Ce^{A_1t}}{-d - Cx_1^*(t)}$$

Let $H_1(t) = e^{At} + (x_0^*(t) - x_1^*)w_1(t)$, $H_{2a}(t) = e^{A_1t} + (x_1^*(t) - x_0^*)w_{2a}(t)$, and $H_{2b}(t) = e^{A_1t} + (x_1^*(t) + x_0^*)w_{2b}(t)$. Then, for any $\Delta_0 \in S_+ - x_0^*$, $\Delta_1 \in S_d - x_1^*$, and $\Delta_1 \in S_{-d} - x_1^*$, there exist $t_i \in \mathcal{T}_i$, $i = \{1, 2a, 2b\}$, such that

$$\Delta_1 = H_1(t_1)\Delta_0, \quad \Delta_{2a} = H_{2a}(t_{2a})\Delta_1, \quad \Delta_{2b} = H_{2b}(t_{2b})\Delta_1$$

respectively. Such t_i are the switching times associated with Δ_i , $i = \{1, 2a, 2b\}$.

To show that these three impact maps are contracting in some sense, define two quadratic Lyapunov functions on the switching surface S . Let V_1 and V_2 be given by

$$V_i(x) = x'P_i x - 2x'g_i + \alpha_i \quad (18)$$

where $P_i > 0$, for $i = 1, 2$. Global asymptotic stability of the origin follows if there exist $P_i > 0$, g_i , α_i such that

$$\begin{aligned} V_2(\Delta_1) &< V_1(\Delta_0) && \text{for all } \Delta_0 \in S_+ - x_0^* \\ V_1(\Delta_{2a}) &< V_2(\Delta_1) && \text{for all } \Delta_1 \in S_d - x_1^* \\ V_1(-\Delta_{2b}) &< V_2(\Delta_1) && \text{for all } \Delta_1 \in S_{-d} - x_1^* \end{aligned} \quad (19)$$

Note that in (19) we have mapped the point $\Delta_{2b} \in \underline{S}_+ + x_0^*$ into $S_+ - x_0^*$, taking advantage of the symmetry of the system. Let $H_{it} = H_i(t)$ and $w_{it} = w_i(t)$.

Theorem 7.1 *Define*

$$\begin{aligned} R_1(t) &= P_1 - H'_{1t}P_2H_{1t} - 2(g_1 - H'_{1t}g_2)w_{1t} + w'_{1t}\alpha w_{1t} \\ R_{2a}(t) &= P_2 - H'_{2at}P_1H_{2at} - 2(g_2 - H'_{2at}g_1)w_{2at} - w'_{2at}\alpha w_{2at} \\ R_{2b}(t) &= P_2 - H'_{2bt}P_1H_{2bt} - 2(g_2 + H'_{2bt}g_1)w_{2bt} - w'_{2bt}\alpha w_{2bt} \end{aligned}$$

where $\alpha = \alpha_1 - \alpha_2$. The origin of the SAT is globally asymptotically stable if there exist $P_1, P_2 > 0$ and g_1, g_2, α such that

$$\begin{cases} R_1(t_1) > 0 & \text{on } S_{t_1} - x_0^* \\ R_{2a}(t_{2a}) > 0 & \text{on } S_{t_{2a}} - x_1^* \\ R_{2b}(t_{2b}) > 0 & \text{on } S_{t_{2b}} - x_1^* \end{cases} \quad (20)$$

for all expected switching times $t_1 \in \mathcal{T}_1$, $t_{2a} \in \mathcal{T}_{2a}$, and $t_{2b} \in \mathcal{T}_{2b}$.

As in corollaries 4.1 and 6.1, a relaxation of the constraints on Δ_0 and Δ_1 in the previous theorem results in computationally efficient conditions.

Corollary 7.1 *The origin of the SAT is globally asymptotically stable if there exist $P_1, P_2 > 0$ and g_1, g_2, α such that*

$$\begin{cases} R_1(t_1) > 0 & \text{on } S - x_0^* \\ R_{2a}(t_{2a}) > 0 & \text{on } S - x_1^* \\ R_{2b}(t_{2b}) > 0 & \text{on } S - x_1^* \end{cases} \quad (21)$$

for all expected switching times $t_1 \in \mathcal{T}_1$, $t_{2a} \in \mathcal{T}_{2a}$, and $t_{2b} \in \mathcal{T}_{2b}$.

For each t_1, t_{2a}, t_{2b} , these conditions are LMIs which can be solved for $P_1, P_2 > 0$ and g_1, g_2, α using efficient available software. As we will see in the next section, although these conditions are more conservative than the ones in theorem 7.1, they are already enough to prove global asymptotic stability of many important SAT.

Note that in many cases, conditions (20) and (21) do not need to be satisfied for all expected switching times. Appendix B shows that bounds on the expected switching times can be obtained when A is Hurwitz. Basically, since $|u| \leq d$ is a bounded input, there exists a bounded set such that any trajectory will eventually enter and stay there. This will lead to bounds on the difference between any two consecutive switching times. Let t_{i-} and t_{i+} , $i = 1, 2a, 2b$, be bounds on the minimum and maximum switching times of the associated impact maps. The expected switching times \mathcal{T}_i can, in general, be reduced to a smaller set (t_{i-}, t_{i+}) . Conditions (20) and (21) can then be relaxed to be satisfied only on (t_{i-}, t_{i+}) instead on all $t_i \in \mathcal{T}_i$. See appendix B for details.

7.4 Examples

The following examples were processed in `matlab` code. The latest version of this software is available at [7]. Before we present the examples, we briefly explain the `matlab` function we developed. The input to this function is a transfer function of an LTI system together with a parameter $d > 0$. If the SAT is proven globally stable, the `matlab` function returns the parameters of the two quadratic surface Lyapunov functions (18). We then confirm conditions (21) are satisfied by plotting the minimum eigenvalues of each $R_i(t)$ on (t_{i-}, t_{i+}) , and showing that these are indeed positive in those intervals.

Example 7.1 Consider the SAT on the left of figure 16 with $d = 1$. It is easy to see the origin of this system is locally stable. The question is if the the origin is also globally asymptotically stable.

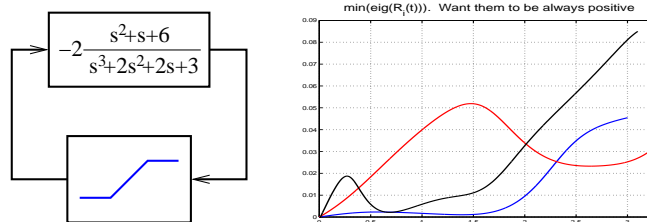


Figure 16: 3rd-order system with unstable nonlinearity sector

Using conditions (21), we show that the origin is in fact asymptotically globally stable. The right side of figure 16 illustrates this fact: the minimum eigenvalue of each condition (21)

is positive on its respective set of expected switching times. The expected switching times in this example are approximately $\mathcal{T}_1 = (0, 3)$, $\mathcal{T}_{2a} = (0, 3.3)$, and $\mathcal{T}_{2b} = (0, 3.1)$. For instance, if $t_1 \geq 3$, there is no point in S_+ with switching time equal to t_1 .

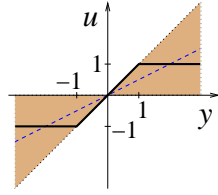


Figure 17: Saturation controller versus constant gain of $1/2$ (dashed)

Note that this system has an unstable nonlinearity sector. If the saturation is replaced by a linear constant gain of $1/2$, the system becomes unstable (see figure 17). This is very interesting since it tells us that classical analysis tools like small gain theorem, Popov criterion, Zames–Falb criterion, and integral quadratic constraints, fail to analyze SAT of this nature. ■

Example 7.2 Consider the SAT in figure 18 with $d = 1$ and $k > 0$. The origin of the SAT is locally stable for any $k > 0$.

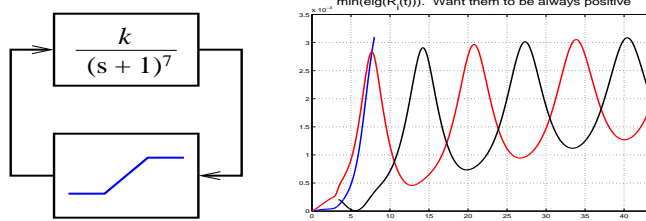


Figure 18: System with relative degree 7 (left); global stability analysis when $k = 2$ (right)

As seen in example 6.2, $\|Ce^{At}B\|_{\mathcal{L}_1} = k$, and the small gain theorem can only be applied when $k < 1$.

Let $k = 2$. The right side of figure 18 shows how conditions (21) are satisfied in some intervals (t_{i-}, t_{i+}) , $i = 1, 2a, 2b$. The intervals (t_{i-}, t_{i+}) are bounds on the expected switching times. Such bounds are such that if conditions (21) are satisfied on (t_{i-}, t_{i+}) , then the system is globally asymptotically stable. For details on how to find these bounds see appendix B. ■

Example 7.3 Consider the SAT in figure 19 with $d = 1$. This system is globally asymptotically stable. This can be proven by direct application of the Popov criterion (see, for example, [11, pages 419–420]). What is interesting about this example is that the system is not exponentially stable. Thus, the method of analysis using piecewise quadratic Lyapunov functions [9] fails to analyze the system.

Quadratic surface Lyapunov functions can, however, be used to analyze and prove global asymptotic stability of the system. The right side of figure 19 shows how conditions (21) are satisfied in some intervals (t_{i-}, t_{i+}) , $i = 1, 2a, 2b$. It is important to notice that these intervals cannot be found as in the previous examples or as explained in appendix B. The reason is that here A is not Hurwitz. Thus, a bounded invariant set cannot be guaranteed as in appendix B. Alternatively, the analysis must be done for all $t_i \geq 0$. The idea of proof is the following: analysis near the origin is done as in appendix A.2. For large values of t_i ,

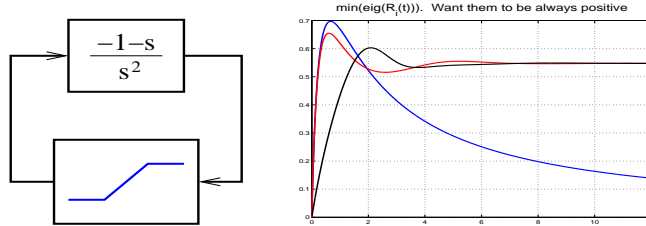


Figure 19: Second order system not exponentially stable

analysis can be as in appendix A.3 for impact maps *2a* and *2b* since the matrix A_1 is stable. For impact map 1, it is required some further analysis. The constraint $P_1 = P_2$ implies that $R_1(\infty) = 0$, which is a requirement since the system is not exponentially stable. For a large enough t_{1+} , it can be shown that $R_1(t) > 0$ for all $t \geq t_{1+}$. The idea here is to show that $\dot{R}_1(t) < 0$ for all $t \geq t_{1+}$. ■

8 Improvement of stability conditions

It is possible to improve condition (8), and consequently conditions (15) and (21), at a cost of increased computations. This section explains how to approximate condition (7) with a less conservative set of LMIs than (8).

8.1 Meaning of condition (7)

As seen in several examples in sections 6 and 7, although condition (8) is more conservative than (7), this is enough to prove global asymptotic stability of many important systems. There are, however, examples where (8) fails to prove stability [6]. Condition (8) only takes into account that $\Delta_0 \in S_0 - x_0^*$, independently of the value of $t \in \mathcal{T}$. Condition (7), however, uses the information that, for a given $t \in \mathcal{T}$, $\Delta_0 \in S_t - x_0^*$. Note that the set S_t has one dimension less than S_0 .

The problem with condition (7) is that, in general, the set S_t is not easily characterized. Let's first see what exactly is condition (7). For every $t \in \mathcal{T}$, we need $\Delta_0' R(t) \Delta_0 > 0$ for all $\Delta_0 \in S_t$, or equivalently, that

$$\begin{cases} \Delta_0 \in \{x \in S_0 \mid x \text{ can be reached by some trajectory of the PLS}\} - x_0^* \\ C_1 H(t) \Delta_0 = 0 \\ x(\tau) \in \bar{X}, \text{ for all } \tau \in [0, t] \end{cases} \quad (22)$$

Next, we explain in detail each constraint in (22), starting with the first inclusion.

The switching surfaces S_0 and S_1 , together with (1), are part of some PLS. The set S_0^d can exclude those points in S_0 that cannot be reached by a trajectory of the PLS starting somewhere in $\mathbb{R}^n \setminus S_0$, since such points play no role in the stability analysis of the system.

Example 8.1 Figure 20 shows a PLS with both switching surfaces S_0 and S_1 , and X defined between them. Above the switching surface S_0 we have system $\dot{x} = A_1 x + B_1$. In the figure we see the vector fields of systems $\dot{x} = A_1 x + B_1$ and (1) along the switching surface S_0 (above and below, respectively), and the vector field of (1) along the switching surface S_1 . The points \bar{x}_0 , \bar{x}_1 , and \bar{x}_2 are the points where $C_0(A_1 \bar{x}_0 + B_1) = 0$, $C_0(A \bar{x}_1 + B) = 0$, and $C_1(A \bar{x}_2 + B) = 0$. Note that \bar{x}_1 must be to the left of \bar{x}_0 in order to guarantee existence of solutions.

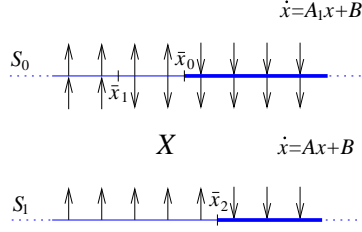


Figure 20: $S_0^d \subset S_0$ and $S_1^a \subset S_1$ are some sets defined to the right of \bar{x}_0 and \bar{x}_2 , respectively

As seen in figure 20, points to the left of \bar{x}_1 do not belong to the domain of the impact map from S_0 to S_1 . Also, points in S_0 between \bar{x}_0 and \bar{x}_1 cannot be reached by any trajectory starting somewhere in $\mathbb{R}^n \setminus S_0$. Thus, only points to the right of \bar{x}_0 need to be considered for stability analysis purposes. Note that those are exactly the points that can be reached by system $\dot{x} = A_1x + B_1$. Similarly, only some points to the right of \bar{x}_2 can be reached by (1). Hence, $S_1^a \subset S_1$ is some set defined to the right of \bar{x}_2 . ■

The first inclusion in (22) is then composed of a linear equality together with a set of linear inequalities. The equality, $C_0\Delta_0 = 0$, comes from the fact that $\Delta_0 \in S_0 - x_0^*$. As for the inequalities, they are necessary to ensure that every point in S_0^d can be reached by some trajectory of the PLS, starting somewhere in $\mathbb{R}^n \setminus S_0$. Such points in S_0 are those where the vector field along S_0 points inward, for each system i that shares a boundary with X through S_0 (thicker segments of line in S_0 in figure 21). As in the left of figure 21, assume C'_0 orientation points toward X (if this is not the case, just consider $-C'_0$ and $-d_0$). The set of points in S_0 where the vector field of system i is parallel to S_0 are those where $C_0\dot{x} = 0$, i.e., $C_0(A_ix + B_i) = 0$, $x \in S_0$. Thus, the set of points in S_0 that can be reached by system i is some subset of the set of points such that $C_0(A_ix + B_i) > 0$, $x \in S_0$.

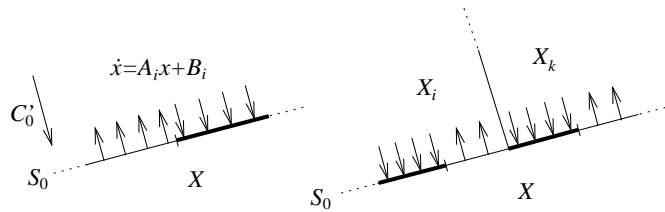


Figure 21: Points in S_0 that can be reached by trajectories of the system

The equality in (22) arises from the fact that $\Delta_1 \in S_1 - x_1^*$, i.e., $C_1\Delta_1 = 0$. In terms of Δ_0 , we have equality (3), that we repeat here

$$C_1 e^{At} \Delta_0 = d_1 - C_1 x_0^*(t) \quad (23)$$

This equality automatically excludes those points in S_0 that do not intersect S_1 , since such points do not have a finite solution $t > 0$ satisfying (23). Note that (23) depends on $t \in \mathcal{T}$, contrasting with the first equality $C_0\Delta_0 = 0$, which is independent of t .

The last inclusion in (22) ensures that a trajectory $x(\tau)$, starting at some point in S_0 , stays in the closure of X , i.e., in \bar{X} , for all $\tau \in [0, t]$. Thus, the first switch must occur at S_1 (see figure 22). The inclusion consists of several infinite dimensional sets of linear inequalities, one for each boundary of X . For instance, in figure 22, it must be true that $C_j x(\tau) \geq d_j$, $j = 0, 1, 2$, for all $\tau \in [0, t]$, assuming C'_j orientations point toward X , as in the figure.

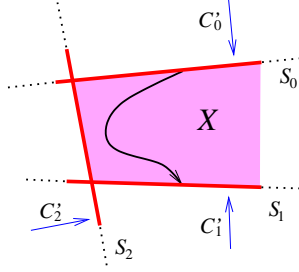


Figure 22: Trajectories starting at S_0 must remain in X

8.2 Less conservative conditions

It was clear from the above description of the set S_t why condition (7) cannot, in general, be written as an equivalent set of LMIs. Basically, the characterization of the set S_t is too complicated. A straightforward transformation of (7) into a set of LMIs was to use only equality $C_0\Delta_0 = 0$. This resulted in a more conservative condition (8). To reduce the conservatism, other inequalities can be incorporate using the S-procedure [1]. The problem is that the S-procedure only results in equivalent, and therefore non-conservative conditions when a quadratic function is subject to a single quadratic constraint. Next, using the S-procedure, we show how equality (23) plus other inequalities can be used to approximate (7) with a set of LMIs. We start by incorporating a single inequality.

First, we approximate S_t with a larger set. For a given $t \in \mathcal{T}$, let $\tilde{S}_t \supset S_t$ be the set of points in S_0 where $C_1x(t) = d_1$. This can be obtained from (23) yielding

$$\tilde{S}_t = \left\{ x_0^* + \Delta_0 \in S_0 : C_1e^{At}\Delta_0 = d_1 - C_1x_0^*(t) \right\} \quad (24)$$

To see the differences between S_t and \tilde{S}_t , consider again example 3.1. Figure 23 shows the solution $C_1x(t)$ for two different initial conditions in S_0^d .

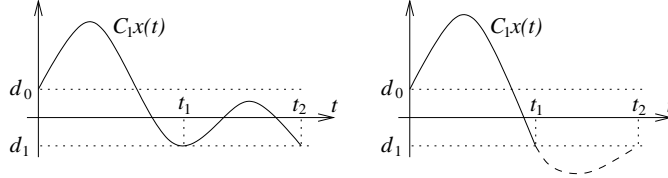


Figure 23: On the left: $C_1x(t) \geq d_1$ for $0 \leq t \leq t_2$; on the right: $C_1x(t) < d_1$ for $t_1 < t < t_2$

On the left of figure 23, $t_{\Delta_0} = \{t_1, t_2\}$. This means $x_0^* + \Delta_0$ belongs to both S_{t_1} , and S_{t_2} . The right side of figure 23 shows what would have happened to $C_1x(t)$ if the switching surface S_1 was not present and no switch had occurred at t_1 . In that case, it would have resulted in the dashed curve in the figure, intersecting S_1 again at $t = t_2$. This means that although t_2 is a solution of (23), it is not a valid switching time since $C_1x(t) < d_1$ for $t_1 < t < t_2$. In other words, the switching time t_2 does not satisfy the inequality $C_1x(t) \geq d_1$ on $[0, t_2]$. Although both t_1 and t_2 satisfy (23), only t_1 is a valid switching time, i.e., $t_{\Delta_0} = \{t_1\}$. Thus, $x_0^* + \Delta_0$ belongs to \tilde{S}_{t_1} , S_{t_1} , and \tilde{S}_{t_2} , but not to S_{t_2} .

Since $S_t \subset \tilde{S}_t$, condition (7) holds if there exist $P_1, P_2 > 0, g_1, g_2, \alpha$ such that

$$R(t) > 0 \quad \text{on } \tilde{S}_t - x_0^* \quad (25)$$

for all expected switching times $t \in \mathcal{T}$. In order to transform this matrix inequality into a set of LMIs, we need to better characterize the set \tilde{S}_t . For that, we are going to use

one inequality from (22) together with equality (23). As discussed above, there are many inequalities to choose from. For the purpose of demonstrating the procedure, assume we choose one of these inequalities, represented here by some L and m such that $L\Delta_0 > m$. In section 8.3, we give an example on how to pick one of these inequalities. A less conservative condition than (25) is then

$$R(t) > 0 \quad \text{on} \quad \left(\tilde{S}_t \cap \{x_0^* + \Delta_0 \mid L\Delta_0 > m\} \right) - x_0^* \quad (26)$$

for all expected switching times $t \in \mathcal{T}$ (see figure 24).

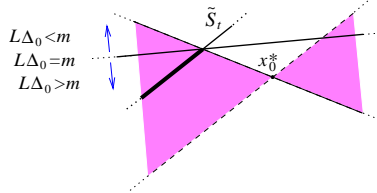


Figure 24: Region in S_0 defined by equality (23) and the inequality $L\Delta_0 > m$ satisfies a conic relation

As seen in figure 24, $\Delta_0 \in \left(\tilde{S}_t \cap \{x_0^* + \Delta_0 \mid L\Delta_0 > m\} \right) - x_0^*$ satisfies a conic relation $\Delta_0' \beta_t \Delta_0 > 0$, for some matrix β_t (the construction of this matrix will be addressed in appendix C). Using the S-procedure, condition (26) is equivalent to

$$R(t) - \tau_t \beta_t > 0 \quad \text{on} \quad S_0 - x_0^* \quad (27)$$

for some scalar function $\tau_t > 0$, and for all expected switching times $t \in \mathcal{T}$. Note that, for each t , (27) is now an LMI.

It is still possible to improve conditions (27) further more. They do not take advantage of all other inequalities, including all of those arising from the last inclusion in (22). In order to guarantee, for instance, that $x(\tau) \in \bar{X}$ on $[0, t]$, it is necessary that the trajectory $x(\tau)$ stays to the correct side of all switching surfaces that compose the boundary X . In particular, it must be true that $C_1 x(\tau) \geq d_1$ for all $\tau \in [0, t]$, i.e.,

$$C_1 \left(e^{A\tau} \Delta_0 + x_0^*(\tau) \right) \geq d_1$$

for all $\tau \in [0, t]$. This is an infinite dimensional set of linear inequalities. To overcome this difficulty, we consider a finite number of values of τ in $[0, t]$. For example, at $\tau = t/2$, we have the following linear constraint on Δ_0 :

$$C_1 e^{At/2} \Delta_0 \geq d_1 - C_1 x_0^*(t/2)$$

As before, this inequality together with \tilde{S}_t satisfies a conic relation $\Delta_0' \gamma_{t/2} \Delta_0 > 0$ in which (27) would be improved to

$$R(t) - \tau_t \beta_t - \tau_{1t} \gamma_{t/2} > 0 \quad \text{on} \quad S_0 - x_0^* \quad (28)$$

for some scalar function $\tau_{1t} > 0$, and for all expected switching times $t \in \mathcal{T}$.

There is an infinite number of constraints that can be added to condition (28) in order to further reduce the level of conservatism. On one hand, the more constraints, the less conservative conditions we get and, in turn, better chances of finding quadratic surface Lyapunov functions (5). On the other hand, increasing the number of constraints will eventually make the problem computationally intractable. It is interesting to notice, however, that many important PLS are analyzed with just conditions of the form of (8), as seen in [6], and sections 6 and 7.

8.3 Application to on/off

Next, we explain how the ideas discussed in the previous section can be used to derive less conservative conditions than (15) for on/off systems, similar to those obtained in (27) and (28). Note that all the ideas discussed in this subsection apply analogously to saturation systems.

Define the sets $\tilde{S}_{t_i} \supset S_{t_i}$, $i = 1, 2$, as in (24). In the case of OFS these are $\tilde{S}_{t_1} = \{x_0^* + \Delta_0 \in S : w_{1t}\Delta_0 = 1\}$ and $\tilde{S}_{t_2} = \{x_1^* + \Delta_1 \in S : w_{2t}\Delta_1 = 1\}$.

Note that the domain of impact map 1 is S_+ . This set is characterized by all points in $x \in S$ such that $CAx \geq 0$. Similarly, the domain of impact map 2 is a subset of S_- . The set S_- is characterized by all points in $x \in S$ such that $CAx \leq 0$. Therefore, conditions (14) hold if there exist $P_1, P_2 > 0$, g_1, g_2 , α such that

$$\begin{cases} R_1(t_1) > 0 & \text{on } \left(\tilde{S}_{t_1} \cap \{x \mid CAx > 0\} \right) - x_0^* \\ R_2(t_2) > 0 & \text{on } \left(\tilde{S}_{t_2} \cap \{x \mid CAx < 0\} \right) - x_1^* \end{cases} \quad (29)$$

for all expected switching times t_1, t_2 , which are less conservative conditions than (15).

As explained in previous sections, Δ_i satisfies a conic relation $\Delta_i' \beta_{t_i} \Delta_i > 0$, for some matrices β_{t_i} (see appendix C for details on the construction of such matrices). Using the S-procedure we obtain equivalent conditions to (29)

$$\begin{cases} R_1(t_1) - \tau_{t_1} \beta_{t_1} > 0 & \text{on } S - x_0^* \\ R_2(t_2) - \tau_{t_2} \beta_{t_2} > 0 & \text{on } S - x_1^* \end{cases} \quad (30)$$

for some $P_i > 0$, g_i , α , some scalar functions $\tau_{t_i} > 0$, and for all expected switching times t_i . For each t_1, t_2 these conditions are LMI which again can be solved using efficient available software. Note that these conditions can still be further improved as in (28).

9 Conclusions

Motivated by the need of new and alternative global analysis tools for certain classes of hybrid systems, this paper developed an entirely new constructive analysis methodology for PLS using *impact maps* and *quadratic surface Lyapunov functions* (SuLF). This methodology consists of inferring global properties of PLS solely by studying their behavior at switching surfaces. The main idea is to efficiently construct SuLF to show that impact maps associated with the PLS are contracting in some sense. The success and power of this new methodology has been demonstrated in globally analyzing equilibrium points and limit cycles of several classes of PLS: relay feedback systems, on/off systems, and saturation systems. A large number of examples of these classes of PLS with a locally stable limit cycle or equilibrium point were successfully globally analyzed. In fact, it is still an open problem whether there exists an example with a globally stable limit cycle or equilibrium point that could not be successfully analyzed with this new methodology.

For the classes of systems we considered so far, there were only advantages using SuLF comparing with piecewise quadratic Lyapunov functions [9]. We could analyze limit cycles for relay feedback systems, no extra complexity was added (i.e., no need for extra partitions), worked exactly the same way for any system dimension, and we could prove global asymptotic stability of PLS that were not exponentially stable. There are, however, limitations to SuLF. It is under investigation how to systematically analyze general PLS, which,

at this time, is much simpler in [9]. Also, if a PLS has a large enough number of partitions such that the method in [9] does not require extra partitions to analyze the system, then SuLF does not seem the right tool since the large number of partitions will lead to many impact maps to analyze that, in turn, will have an associated infinite dimensional LMI that needs to be gridded along scalar variables.

A final word to mention that the reason why we chose ‘‘SuLF’’ instead of ‘‘QSuLF’’ (quadratic SuLF) is due to the fact that new tools are emerging that allows the search for polynomial Lyapunov functions to be done by solving a semi-definite program [14]. Thus, future work will allow the use of high dimensional surface Lyapunov functions instead of just quadratic.

Appendix: Technical Details

A Technical details for on/off systems

A.1 Choice of x_0^* and x_1^*

We now explain how we chose x_0^* and x_1^* such that both $Cx_0^*(t) < d$ and $Cx_1^*(t) < d$ for all $t > 0$. We start with x_1^* .

x_1^* is found as explained in section 6.1 (see the right side of figure 8). In this case, $x_1^* \in S^*$ is given by $x_1^* = (P_d^{-1}C'd)/(CP_d^{-1}C')$, where $P_d > 0$ satisfies $P_dA + A'P_d = -I$.

The choice of x_0^* is more tricky since A_1 may be unstable. If A_1 is stable then we can use the same ideas as we did for x_1^* . First, let $P_u > 0$ satisfy $P_uA_1 + A_1'P_u = -I$. Then

$$x_0^* = (d + cA_1^{-1}B_1) \frac{P_u^{-1}C'}{CP_u^{-1}C'} - A_1^{-1}B_1$$

If A_1 is not stable (but has at least one stable eigenvalue) then we need to find a point in S such this belongs to a stable mode of A_1 . If A_1 has real poles then these must be stable. Let λ be a real eigenvalue of A_1 with associated eigenvector v (assume $Cv \neq 0$). Then, if we find a point in S that only excites this mode, the trajectory $x(t)$ will converge to $-A_1^{-1}B_1$ and $Cx(t) < d$ for all $t > 0$. such a point in S is given by

$$x_0^* = -A_1^{-1}B_1 + \frac{d + CA_1^{-1}B_1}{Cv}v$$

In case A_1 only has complex poles, pick a stable complex conjugate pair of eigenvalues $\lambda, \underline{\lambda}$ with associated eigenvectors v, \underline{v} , where \underline{v} stands for the complex conjugate of x . Let, $v_a = v + \underline{v}$ and $v_b = i(v - \underline{v})$. Then, any initial condition starting in the hyperplane defined by $-A_1^{-1}B_1 + \alpha_a v_a + \alpha_b v_b$, $\alpha_a, \alpha_b \in \mathbb{R}$ will converge to $-A_1^{-1}B_1$ as time goes to infinity since it only excites this stable complex conjugate mode. An orthogonal basis in this plane can be defined by letting $v_c = -(v_a'v_b)v_a + v_b$. The basis is then given by

$$V = \begin{bmatrix} v_a & v_c \\ \|v_a\| & \|v_c\| \end{bmatrix}$$

The trajectory in this basis satisfies $\dot{\alpha} = V'A_1V\alpha = A_v\alpha$. We need to find an α_0 such that $C(-A_1^{-1}B_1 + V\alpha_0) = d$ and $C(-A_1^{-1}B_1 + V\alpha(t)) < d$ for all $t > 0$. This is a similar problem to the one we dealt above when finding x_1^* . In this case, α_0 is given by

$$\alpha_0 = \frac{d + CA_1^{-1}B_1}{CVP_v^{-1}V'C'}P_v^{-1}V'C'$$

where $P_v > 0$ satisfies $P_v A_v + A'_v P_v = -I$. Finally, $x_0^* = -A_1^{-1} B_1 + V \alpha_0$.

If A_1 only has complex unstable eigenvalues, then for any choice of x_0^* , $Cx(t) = d$ will have an infinity number of solutions for $t > 0$. In this case, x_0^* must be chosen such that the smallest solution $t > 0$ of $Cx(t) = d$ is higher than the maximum possible expected switching time. Note that such x_0^* may not exist. If that is the case, the linearization of the impact map must be parametrized by another variable at those values of $t \in \mathcal{T}$ where $Cx(t) = d$, as explained in section 3.

A.2 Constraints imposed when $t_i = 0$

As seen in section 6.4, when $t_i = 0$, $V_1(\Delta_0) = V_2(\Delta_1)$, for all Δ_0, Δ_1 such that $CA(x_0^* + \Delta_0) = CA(x_1^* + \Delta_1) = 0$ and $C\Delta_0 = C\Delta_1 = 0$. This is equivalent to have $R_0 = R_1(0) = R_2(0) = 0$. Since analyzing $R_1(t)$ or $R_2(t)$ near zero will lead to the same results, we analyze $R_1(t)$ at $t = 0$. From section 6.3, $R_0 = R_1(0)$ is given by

$$R_0 = P_1 - P_2 - (g_1 + P_2 v_0 - g_2) w - w' (g_1 + P_2 v_0 - g_2)' + w' w (\alpha + 2v_0' g_2 - v_0' P_2 v_0)$$

where $v_0 = x_0^* - x_1^*$ and

$$w \Delta_0 = \lim_{t \rightarrow 0} w_1(t) \Delta_0 = -\frac{CA}{C(Ax_0^* + Bd)} \Delta_0$$

Let $l \in w^{\perp 5}$, $z = w'/(ww')$, and $P = P_1 - P_2$. Since $R_0 = 0$, then $l'R_0 l = l'Pl = 0$. This means that in the basis (l, z) , the matrix P must have the following structure

$$P_F = \begin{pmatrix} 0 & \Gamma_1 \\ \Gamma_1' & \Gamma_2 \end{pmatrix}$$

for some $\Gamma_1 \in \mathbb{R}^{n-1}$ and $\Gamma_2 \in \mathbb{R}$. Thus, $P = FP_F F'$, where $F = [l \ z]$. Therefore, once $P_2 > 0$ is fixed, $P_1 > 0$ must satisfy $P_1 = FP_F F' + P_2$. The same way $l'R_0 z = 0$, or $l'(Pz - g_1 - P_2 v_0 + g_2) = 0$. Hence, $Pz - g_1 - P_2 v_0 + g_2 = kz$ for some $k \in \mathbb{R}$. For a given g_2 , g_1 is then given by

$$g_1 = (P_1 - P_2)z - P_2 v_0 + g_2 - kz$$

Finally, it must be true that $z'R_0 z = 0$ leading to

$$\alpha = -z'(P_1 - P_2)z + 2z'(g_1 + P_2 v_0 - g_2) + v_0' P_2 v_0 - 2v_0' g_2$$

In conclusion, the constraints imposed when $t_i = 0$ reduce the free variable in conditions (14) and (15) to $P_2, \Gamma_1, \Gamma_2, g_2$, and k .

A.3 Checking stability conditions for $t_i > t_{imax}$

For simplicity, we are going to present the case when $d = 0$. The other cases follow analogously. Assume conditions (16) are satisfied for all $t_i \leq t_{imax}$. We would like to easily check if they will also be satisfied for all $t_i > t_{imax}$. Let's first concentrate on condition

$$l'_{t_2} \Pi' e^{A't_2} P_1 e^{At_2} \Pi l_{t_2} < l'_{t_2} \Pi' P_2 \Pi l_{t_2}$$

⁵ w^\perp are the *orthogonal complements* to w , i.e., matrices with a maximal number of column vectors forming an orthonormal set such that $w'w^\perp = 0$.

It is sufficient to show that

$$\Pi' e^{A't_2} \Pi Q_1 \Pi' e^{At_2} \Pi < Q_2$$

for all $t > t_{2max}$, and where $Q_i = \Pi' P_i \Pi$. Next, we find an upper bound on the left side of the last inequality. Let $A_z = \Pi' A \Pi$. Since A is a stable matrix, it is possible to find a Q and a $\lambda > 0$ such that $Q A_z + A_z' Q < -\lambda Q$. This in turn implies that $z'(t) Q z(t) < e^{-\lambda t} z_0' Q z_0$, where $z(t)$ is the solution of $\dot{z} = A_z z$ with initial condition z_0 . Using the fact that $e^{A_z t} = \Pi' e^{At} \Pi$, we have

$$z_0' \Pi' e^{A't_2} \Pi Q \Pi' e^{At_2} \Pi z_0 < e^{-\lambda t} z_0' Q z_0$$

or simply

$$\Pi' e^{A't_2} \Pi Q \Pi' e^{At_2} \Pi < e^{-\lambda t} Q$$

Hence, for some k

$$\begin{aligned} \Pi' e^{A't_2} \Pi Q_1 \Pi' e^{At_2} \Pi &< \Pi' e^{A't_2} \Pi k Q \Pi' e^{At_2} \Pi \\ &< k e^{-\lambda t} Q \\ &< k e^{-\lambda t_{2max}} Q \end{aligned}$$

Therefore, we need to guarantee $k e^{-\lambda t_{2max}} Q < Q_2$. Note that we want to chose the largest λ and the smallest k .

If A_1 is stable, a similar condition can be found analogously. If A_1 (and also A if $d = 0$) has unstable complex poles, however, this approach will not work since $e^{A_1 t}$ is unbounded when $t \rightarrow \infty$. In such cases, it is fundamental to get an upper bound on t_{1max} . How to find such bound is currently under investigation.

B Technical details for saturation systems: bounds on switching times

In this section, we will talk about computational aspects related to finding $P_i > 0$, g_i , and α in (20) or (21). For many SAT, the sets of expected switching times are $[0, \infty)$. Computationally, in general, it is impossible to check directly if the stability conditions (20) or (21) are satisfied for all expected switching times. An alternative is to find some intervals (t_{i-}, t_{i+}) such that if (20) or (21) are satisfied in those intervals, then stability follows. Notice there are many ways to finds such bounds, and the method we propose here is not unique.

In [6], we showed that in the case of relay feedback systems, there is a bounded invariant set where every trajectory will eventually enter. Hence, bounds on the expected switching times could be found by computing bounds on switching times of trajectories inside that bounded invariant set. This same idea can be used here whenever A is Hurwitz. In fact, since $u = \pm d$ is a bounded input, a bounded and invariant set such that any trajectory will eventually enter can be found. This will lead to bounds on the difference between any two consecutive switching times. This way, the search for $P_i > 0$, g_i , and α in (21) and (21) becomes restricted to $0 \leq t_{i-} < t < t_{i+} < \infty$, $i = 1, 2a, 2b$.

First, notice that $t_{1-} = t_{2a-} = 0$ since the associated impact maps are defined on the same switching surface and are allowed to have zero switching time. Analysis of impact maps 1 and 2a at $t_i = 0$ imposes the same constraints on the parameters of the Lyapunov functions as in OFS. See appendix A.2 for details.

As for impact map $\Delta_1 \rightarrow \Delta_{2b}$, zero switching never occurs since there is a “gap” between S and \underline{S} , resulting in a nonzero switching time for every trajectory starting in S_{-d} . For certain large values of $\|\Delta_1\|$, the switching times can be made arbitrarily small. In the invariant bounded set described above, however, switching times for the impact map $2b$ cannot be made arbitrarily small, and a lower bound t_{2b-} can be found. Using the same ideas, upper bounds on expected switching times for all impact maps can be found. Bounds on switching times for the case where A has unstable imaginary eigenvalues can be found as explained in example 7.3.

Before finding bounds on expected switching times, we need to characterize a bounded set such that any trajectory will eventually enter and stay there. The following proposition is similar to [6, proposition 7.1]. Thus, the proof is omitted here.

Proposition B.1 *Consider the system $\dot{x} = Ax + Bu$, $y = Fx$, where A is Hurwitz, $u(t) = \pm d$, and F is a row vector. Then*

$$\limsup_{t \rightarrow \infty} |Fx(t)| \leq d \|Fe^{At}B\|_{\mathcal{L}_1}$$

Remember that, by definition, $\|Fe^{At}B\|_{\mathcal{L}_1}$ is given by

$$\|Fe^{At}B\|_{\mathcal{L}_1} = \int_0^\infty |Fe^{At}B| dt$$

As a remark, if $F = C$ and $\|Fe^{At}B\|_{\mathcal{L}_1} < 1$, it follows the origin is globally asymptotically stable. When $\limsup_{t \rightarrow \infty} |Cx(t)| < d$, eventually all trajectories enter and remain in the set $\{x \mid |Cx| < d\}$, where the system is linear and stable. Note that this remark also follows from the well known small-gain theorem.

We first focus our attention on upper bounds of the switching times t_{i+} , starting with t_{1+} . A trajectory $x(t)$ starting at $x_0 \in S_+$ is given by $x(t) = e^{At}(x_0 + A^{-1}Bd) - A^{-1}Bd$. Thus, the output $y(t) = Cx(t)$ is given by

$$y(t) = Ce^{At}(x_0 + A^{-1}Bd) - CA^{-1}Bd$$

Since we are assuming $-CA^{-1}Bd < d$, and A Hurwitz, it is easy to see that $y(t)$ cannot remain larger than d for all $t > 0$. For any initial condition $x_0 \in S_+$, $Ce^{At}(x_0 + A^{-1}Bd) \rightarrow 0$ as $t \rightarrow \infty$, which means $y(t) = d$ for some t . Thus, a switch must occur in finite time. Since for a sufficiently large enough time t , $x(t)$ enters a bounded invariant set (from the above proposition), an upper bound on this switching time t_{1+} can be obtained. The following proposition is similar to [6, proposition 7.2].

Proposition B.2 *Let $t_{1+} > 0$ be the smallest solution of*

$$\int_{t_{1+}}^\infty |Ce^{At}B| dt + |Ce^{At_{1+}}A^{-1}B| \leq (CA^{-1}B + 1)$$

If t_a and t_b are sufficiently large consecutive switching times of the first impact map then $|t_a - t_b| \leq t_{1+}$.

Next, we find upper bounds on the expected switching times of impact maps $2a$ and $2b$. The idea here is to find the minimum $t_2 \geq 0$ such that $|y(t)| = |Ce^{At}x_0| \leq d$, for all $t \geq t_2$ and all x_0 in the bounded invariant set. In this derivation, $t_{2a+} = t_{2b+} = t_2$.

Proposition B.3 *Let $t_2 > 0$ be the smallest solution of*

$$\int_0^\infty \left| C e^{A_1 t_2} e^{A t} B \right| dt \leq 1 \quad (31)$$

If t_a and t_b are sufficiently large consecutive switching times of impact maps 2a or 2b, then $|t_a - t_b| \leq t_2$, and $t_{2a+} = t_{2b+} = t_2$.

We now focus on the lower bound on the expected switching times of impact map 2b, i.e, t_{2b-} . Remember that if $x_0 \in S_+$, then $y(0) = d$. Since $d > 0$, it must be true that $y(t) > -d$ at least in some interval $(0, \epsilon)$. Basically, the time it takes to go from S to \underline{S} must always be nonzero. The next result shows that when a trajectory enters the bounded invariant set characterized above, ϵ cannot be made arbitrarily small. Thus, a lower bound on the time it takes between two consecutive switches from S to \underline{S} can be obtained.

Proposition B.4 *Let $k_{dd} = \|CA_1^2 e^{A t} B\|_{\mathcal{L}_1}$, and $k_{dl} = \|CA_1 e^{A t} B\|_{\mathcal{L}_1}$ and define $t_{21} = 2/\sqrt{k_{dd}}$, $t_{22} = 2/k_{dl}$. Let $t_{2b-} = \max\{t_{21}, t_{22}\}$. If t_a and t_b are sufficiently large consecutive switching times of impact map 2b, then $|t_a - t_b| \geq t_{2b-}$.*

The proof is similar to the proof of [6, proposition 7.3].

C Construction of conic relations

We now describe how to construct the cones β_t introduced in section 8.2. Remember that for each $t > 0$, the cone is defined by two hyperplanes in S_0 : one is the hyperplane parallel to \tilde{S}_t containing x_0^* and the other is the hyperplane defined by the intersection of $\mathcal{M} = \{x_0^* + \Delta_0 \in S_0 \mid L\Delta_0 = m\}$ and \tilde{S}_t , and containing the point x_0^* (see figure 24). Let $\Pi_0 l_t$ and $\Pi_0 s_t$, respectively, be vectors in S_0 perpendicular to each hyperplane. Once these vectors are known, the cone can easily be characterized. This is composed of all the vectors $\Delta_0 \in S_0 - x_0^*$ such that $\Delta_0' \Pi_0 (s_t l_t' + l_t s_t') \Pi_0' \Delta_0 \geq 0$. The symmetric matrix β_t introduced in (27) is just $\beta_t = \Pi_0 \tilde{\beta}_t \Pi_0'$ where $\tilde{\beta}_t = s_t l_t' + l_t s_t'$. Remember that the cone is centered at x_0^* and note that after l_t is chosen, s_t must have the right direction in order to guarantee $(\tilde{S}_t \cap \{x_0^* + \Delta_0 \mid L\Delta_0 > m\}) \subset \{x_0^* + \Delta_0 \in S_0 \mid \Delta_0' \beta_t \Delta_0 > 0\}$.

We first find $\Pi_0 l_t$, the vector perpendicular to \tilde{S}_t . Looking back at the definition of \tilde{S}_t , l_t is given by

$$l_t = \frac{(C_1 e^{A t} \Pi_0)'}{\|C_1 e^{A t} \Pi_0\|^2} (d_1 - C_1 x_0^*(t))$$

The derivation of s_t is not as trivial as l_t . We actually need to introduce a few extra variables. The first one is $\Pi_0 l_0$, the vector perpendicular to the set \mathcal{M} , given by $l_0 = (L\Pi_0)' m / \|L\Pi_0\|^2$.

Proposition C.1 *The hyperplane defined by the intersection of \mathcal{M} and \tilde{S}_t , and containing the point x_0^* is perpendicular to the vector*

$$\frac{\Pi_0 l_t}{\|l_t\|} \|l_0\| - \frac{\Pi_0 l_0}{\|l_0\|} \|l_t\|$$

Proof: \mathcal{M} can be parameterize the following way

$$\mathcal{M} = \left\{ x_0^* + \Delta_0 \in S_0 \mid \Delta_0 = \Pi_0 (l_0 + l_0^\perp z), z \in \mathbb{R}^{n-2} \right\}$$

and \tilde{S}_t

$$\tilde{S}_t = \{x_0^* + \Delta_0 \in S_0 \mid \Delta_0 = \Pi_0(l_t + l_t^\perp w), w \in \mathbb{R}^{n-2}\}$$

The intersection of \mathcal{M} and \tilde{S}_t occurs at points in S_0 such that $l_0 + l_0^\perp z = l_t + l_t^\perp w$. Multiplying on the left by l_t' we have $l_t' l_0 + l_t' l_0^\perp z = l_t' l_t$ or

$$l_t' l_0^\perp z = \|l_t\|^2 - l_t' l_0 \quad (32)$$

We want to show that

$$\left(\frac{l_t}{\|l_t\|} \|l_0\| - \frac{l_0}{\|l_0\|} \|l_t\| \right)' (l_0 + l_0^\perp z) = 0$$

Using (32) we have

$$\begin{aligned} \left(\frac{l_t}{\|l_t\|} \|l_0\| - \frac{l_0}{\|l_0\|} \|l_t\| \right)' (l_0 + l_0^\perp z) &= \frac{l_t' l_0}{\|l_t\|} \|l_0\| + \frac{l_t' l_0^\perp z}{\|l_t\|} \|l_0\| - \frac{l_0' l_0}{\|l_0\|} \|l_t\| \\ &= \frac{l_t' l_0}{\|l_t\|} \|l_0\| + \frac{\|l_t\|^2 - l_t' l_0}{\|l_t\|} \|l_0\| - \|l_0\| \|l_t\| \\ &= 0 \end{aligned}$$

■

The characterization of s_t is not complete yet. The orientation of s_t must be carefully chosen to guarantee that the cone \mathcal{C}_t contains $\tilde{S}_t \cap \{x_0^* + \Delta_0 \mid L\Delta_0 > m\}$.

Proposition C.2 *If*

$$s_t = m \left(\frac{l_0}{\|l_0\|} \|l_t\| - \frac{l_t}{\|l_t\|} \|l_0\| \right)$$

then the cone $\{x_0^ + \Delta_0 \in S_0 \mid \Delta_0' \beta_t \Delta_0 > 0\}$ contains $\tilde{S}_t \cap \{x_0^* + \Delta_0 \mid L\Delta_0 > m\}$.*

The proof, omitted here, is based on taking a point $\Delta_0 \in (\tilde{S}_t \cap \{x_0^* + \Delta_0 \mid L\Delta_0 > m\}) - x^*$ and showing that $\Delta_0' \beta_t \Delta_0 > 0$.

References

- [1] S. Boyd, L. El Ghaoui, Eric Feron, and V. Balakrishnan. *Linear Matrix Inequalities in System and Control Theory*. SIAM, Philadelphia, 1994.
- [2] M. S. Branicky. *Studies in Hybrid Systems: Modeling, Analysis, and Control*. PhD thesis, Massachusetts Institute of Technology, 1995.
- [3] Fernando D'Amato, Alexandre Megretski, Ulf Jönsson, and M. Rotea. Integral quadratic constraints for monotonic and slope-restricted diagonal operators. In *ACC*, pages 2375–2379, San Diego, CA, USA, June 1999.
- [4] Jorge M. Gonçalves. *Constructive Global Analysis of Hybrid Systems*. PhD thesis, Massachusetts Institute of Technology, Cambridge, MA, September 2000.
- [5] Jorge M. Gonçalves. \mathcal{L}_2 -gain of double integrators with saturation nonlinearity. *IEEE Transactions on Automatic Control*, 47(12), December 2002.

- [6] Jorge M. Gonçalves, Alexandre Megretski, and Munther A. Dahleh. Global stability of relay feedback systems. *IEEE Transactions on Automatic Control*, 46(4):550–562, April 2001.
- [7] Jorge M. Gonçalves’ web page. <http://web.mit.edu/jmg/www/>.
- [8] Arash Hassibi and Stephen Boyd. Quadratic stabilization and control of piecewise linear systems. In *ACC, Philadelphia, Pennsylvania*, June 1998.
- [9] Mikael Johansson and Anders Rantzer. Computation of piecewise quadratic Lyapunov functions for hybrid systems. *IEEE Transactions on Automatic Control*, 43(4):555–559, April 1998.
- [10] Ulf Jönsson and Alexandre Megretski. The Zames–Falb IQC for systems with integrators. *IEEE Transactions on Automatic Control*, 45(3):560–565, March 2000.
- [11] Hassan K. Khalil. *Nonlinear Systems*. Prentice Hall, N.J., 2nd edition, 1996.
- [12] Alexandre Megretski. New IQC for quasi-concave nonlinearities. In *ACC, San Diego, California*, June 1999.
- [13] Alexandre Megretski and Anders Rantzer. System analysis via integral quadratic constraints. *IEEE Transactions on Automatic Control*, 42(6):819–830, June 1997.
- [14] Pablo A. Parrilo. *Structured Semidefinite Programs and Semialgebraic Geometry Methods in Robustness and Optimization*. PhD thesis, California Institute of Technology, Pasadena, CA, 2000.
- [15] Stefan Pettersson and Bengt Lennartson. An LMI approach for stability analysis of nonlinear systems. In *ECC, Brussels, Belgium*, July 1997.
- [16] Ali Saberi, Zongli Lin, and Andrew Teel. Control of linear systems with saturating actuators. *IEEE Transactions on Automatic Control*, 41(3):368–378, March 1996.
- [17] Rodolfo Suárez, José Alvarez, and Jesús Alvarez. Linear systems with single saturated input: stability analysis. In *30th CDC, Brighton, England*, December 1991.
- [18] Héctor J. Sussmann, Eduardo D. Sontag, and Yudi Yang. A general result on the stabilization of linear systems using bounded controls. *IEEE Transactions on Automatic Control*, 39(12):2411–2425, December 1994.
- [19] Andrew R. Teel. A nonlinear small gain theorem for the analysis of control systems with saturation. *IEEE Transactions on Automatic Control*, 41(9):1256–1270, September 1996.
- [20] G. Zames and P. L. Falb. Stability conditions for systems with monotone and slope-restricted nonlinearities. *SIAM Journal of Control*, 6(1):89–108, 1968.